JOURNAL OF VIROLOGY, Feb. 2010, p. 1221–1236 Vol. 84, No. 3
0022-538X/10/$12.00 doi:10.1128/JVI.02087-09

Immune Evasion Proteins of Murine Cytomegalovirus Preferentially Affect Cell Surface Display of Recently Generated Peptide Presentation Complexes[▽]

Niels A. W. Lemmermann, Kerstin Gergely, Verena Böhm, Petra Deegen, Torsten Däubner, and Matthias J. Reddehase*

Institute for Virology, University Medical Center of the Johannes Gutenberg University, Mainz, Germany

Received 2 October 2009/Accepted 6 November 2009

For recognition of infected cells by CD8 T cells, antigenic peptides are presented at the cell surface, bound to major histocompatibility complex class I (MHC-I) molecules. Downmodulation of cell surface MHC-I molecules is regarded as a hallmark function of cytomegalovirus-encoded immunoevasins. The molecular mechanisms by which immunoevasins interfere with the MHC-I pathway suggest, however, that this downmodulation may be secondary to an interruption of turnover replenishment and that hindrance of the vesicular transport of recently generated peptide-MHC (pMHC) complexes to the cell surface is the actual function of immunoevasins. Here we have used the model of murine cytomegalovirus (mCMV) infection to provide experimental evidence for this hypothesis. To quantitate pMHC complexes at the cell surface after infection in the presence and absence of immunoevasins, we generated the recombinant viruses mCMV-SIINFEKL and mCMV-Δ*m06m152*-SIINFEKL, respectively, expressing the K^b-presented peptide SIINFEKL with early-phase kinetics in place of an immunodominant peptide of the viral carrier protein gp36.5/m164. The data revealed ~10,000 K^b molecules presenting SIINFEKL in the absence of immunoevasins, which is an occupancy of ~10% of all cell surface K^b molecules, whereas immunoevasins reduced this number to almost the detection limit. To selectively evaluate their effect on preexisting pMHC complexes, cells were exogenously loaded with SIINFEKL peptide shortly after infection with mCMV-SIINFEKA, in which endogenous presentation is prevented by an L174A mutation of the C-terminal MHC-I anchor residue. The data suggest that pMHC complexes present at the cell surface in advance of immunoevasin gene expression are downmodulated due to constitutive turnover in the absence of resupply.

CD8 T cells recognize infected cells by interaction of their T-cell receptor (TCR) with a cell surface presentation complex composed of a cognate antigenic peptide bound to a presenting allelic form of a major histocompatibility complex class I (MHC-I) glycoprotein (77, 85, 97, 98). The number of such "peptide receptors" per cell has been estimated to be on the order of 10^5 to 10^6 for each MHC-I allomorph (for a review, see reference 82). Viral antigenic peptides are generated within infected cells by proteolytic processing of viral proteins, usually in the proteasome, and associate with nascent MHC-I proteins in the endoplasmic reticulum (ER) before the peptide-MHC (pMHC) complexes travel to the cell surface with the cellular vesicular flow (for reviews, see references 13, 87, 92, and 93). CD8 T cells have long been known to protect against cytomegalovirus (CMV) infection and disease in animal models (60, 72; reviewed in references 33 and 36) and in humans (9, 61, 67, 75, 76). As shown only recently in the murine CMV (mCMV) model of infection of immunocompromised mice by adoptive transfer of epitope-specific CD8 T cells, antiviral protection against CMV is indeed TCR mediated and epitope dependent. Specifically, memory cells purified by TCR-based epitope-specific cell sorting, as well as cells of a peptide-selected cytolytic T-lymphocyte line, protected against mCMV expressing the cognate antigenic peptide, the IE1 peptide 168-YPHFMPTNL-176 in this example, but failed to control infection with a recombinant mCMV expressing a peptide analogue in which the C-terminal MHC-I anchor residue leucine was replaced with alanine (3).

Interference with the MHC-I pathway of antigen presentation has evolved as a viral immune evasion mechanism of CMVs and other viruses, mediated by virally encoded proteins that inhibit MHC-I trafficking to the cell surface (for reviews, see references 1, 24, 27, 29, 63, 70, 71, 84, and 95). These molecules are known as immunoevasins (50, 70, 89), as "viral proteins interfering with antigen presentation" (VIPRs) (95), or as negative "viral regulators of antigen presentation" (vRAPs) (34). Although the detailed molecular mechanisms differ between different CMV species in their respective hosts, the common biological outcome is the inhibition of antigen presentation. Accordingly, downmodulation of MHC-I cell surface expression is a hallmark of molecular immune evasion and actually led to the discovery of this class of molecules. Since CD8 T cells apparently protect against infection with wild-type CMV strains despite the expression of immunoevasins, the *in vivo* relevance of these molecules is an issue of current interest and investigation (for a review, see reference 14). As shown recently with the murine model, antigen presentation in infected host cells is not completely blocked for all epitopes, because pMHC complexes that are constitutively

* Corresponding author. Mailing address: Institute for Virology, University Medical Center of the Johannes Gutenberg University, Hochhaus am Augustusplatz, 55101 Mainz, Germany. Phone: 49-6131-39-33650. Fax: 49-6131-39-35604. E-mail: Matthias.Reddehase@uni-mainz.de.

▽ Published ahead of print on 11 November 2009.

formed in sufficiently large amounts can exhaust the inhibitory capacity of the immunoevasins (40). Likewise, enhancing antigen processing conditionally with gamma interferon (IFN-γ) aids in peptide presentation in the presence of immunoevasins (18, 28). Thus, by raising the threshold of the amount of peptide required for presentation, immunoevasins determine whether a particular viral peptide can function as a protective epitope—an issue of relevance for rational vaccine design as well (94). Whereas deletion of immunoevasin genes gives only incremental improvement to the control of infection in immunocompetent mice (22, 51), expression of immunoevasins reduces the protective effect of adoptively transferred CD8 T cells in immunocompromised recipients (37, 40, 47, 48). In a bone marrow transplantation model, immunoevasins were recently found to contribute to enhanced and prolonged virus replication during hematopoietic reconstitution and, consequently, also to higher latent viral genome loads in the lungs and a higher incidence of virus recurrence (4). Notably, however, immunoevasins do not inhibit but, rather, enhance CD8 T-cell priming (5, 21, 22, 56), due to higher viral replication levels in draining lymph nodes associated with sustained antigen supply for the cross-priming of CD8 T cells by uninfected antigen-presenting cells (5).

For mCMV, three molecules are proposed to function as vRAPs, only two of which are confirmed negative regulators that downmodulate cell surface MHC-I (34, 62, 89) and inhibit the presentation of antigenic peptides to CD8 T cells (34, 62). Immunoevasin gp40/m152 transiently interacts with MHC-I molecules and mediates their retention in a *cis*-Golgi compartment (96), whereas gp48/m06 stably binds to MHC-I molecules in the ER and mediates sorting of the complexes for lysosomal degradation by a mechanism that involves the cellular cargo sorting adaptor proteins AP1-A and AP3-A (73, 74). The third proposed immunoevasin of mCMV, gp34/m04 (46), also binds stably to MHC-I molecules. A function as a CD8 T-cell immunoevasin was predicted from some alleviation of immune evasion for certain epitopes and MHC-I molecules in cells infected with the deletion mutant mCMV-Δ*m04* (34, 42, 89), but gp34/m04 does not reduce the steady-state level of cell surface class I molecules and does not inhibit peptide presentation when expressed selectively after infection with mCMV-Δ*m06m152* (34, 62). The m04–MHC-I complexes are expressed on the cell surface (46) and appear to be involved in the modulation of natural killer cell activity (45).

Here we give the first report on quantitating the efficacy of immunoevasins in terms of absolute numbers of pMHC complexes displayed at the cell surface. By comparing the fate of pMHC complexes already present at the cell surface in advance of immunoevasin gene expression with that of newly formed pMHC complexes, our data provide direct evidence to conclude that downmodulation of cell surface MHC-I molecules is secondary to an interruption of the flow of newly formed pMHC complexes to the cell surface.

(Part of this work was presented at the 12th International CMV/Betaherpesvirus Workshop, 10 to 14 May 2009, Boston, MA.)

MATERIALS AND METHODS

Generation of recombinant viruses. Recombinant plasmids were constructed according to established procedures, and enzyme reactions were performed as recommended by the manufacturers. Throughout, the fidelity of PCR-based cloning steps was verified by sequencing (GATC, Freiburg, Germany).

(i) Shuttle plasmids for mutagenesis. pST76K-m164_SIINFEKL and pST76K-m164_SIINFEKA were constructed to replace the D^d-restricted antigenic m164 peptide 167-AGPPRYSRI-175 (33, 35, 39) with the K^b-restricted ovalbumin (Ova)-derived peptide SIINFEKL and its nonantigenic analog SIINFEKA. Plasmid pBlue-m164_SIINFEKL was generated as an intermediate. For this purpose, a 1,288-bp AgeI/NcoI fragment carrying the SIINFEKL coding sequence in place of the intrinsic m164 peptide coding sequence was generated via site-directed mutagenesis by overlap extension PCR (31), with plasmid pBlue-m164 (38) as template DNA. The primers were m164_Mut_rev (5′-CGTCCGACGC GCGACGAAGCGTTCG-3′), representing nucleotides (nt) 222,376 to 222,400 (GenBank accession no. NC_004065 [complete genome]), and m164_SIINFEKL_for (5′-**AGTATAATCAACTTTGAAAAAGCG**TTCTGGGCCGTCA ACAACCAG-3′) (nt 222,855 to 222,835; replaced nucleotides for peptide swapping are indicated in bold), as well as m164_SIINFEKL_rev (5′-**CGCTTTTTC AAAGTTGATTATACT**GTCAGCGCCCCACGTCCGAC-3′; nt 222,883 to 222,902) and m164_Mut_for (5′-CCTGACCGGCGATCTGCTGGTCCCG-3′; nt 223,745 to 223,721). In the subsequent fusion reaction, m164_Mut_rev and m164_Mut_for were used as primers. PCR was performed with the following cycler conditions: an initial step for 5 min at 95°C for activation of ProofStart *Taq* DNA polymerase (Qiagen, Hilden, Germany) was followed by 30 cycles of 45 s at 94°C, 60 s at 65°C, and 60 s at 72°C. pBlue-m164 was digested with AgeI and NcoI, and the 1,291-bp AgeI/NcoI fragment was replaced with the PCR-mutated 1,288-bp AgeI/NcoI fragment. Finally, pBlue-m164_SIINFEKL was cleaved with HpaI and SphI, and the resulting 5,241-bp HpaI/SphI fragment was ligated into the SmaI/SphI-cleaved shuttle plasmid pST76-KSR (6, 66). For construction of shuttle plasmid pST76-m164_SIINFEKA, pBlue-m164-SIINFEKA was generated as described above, except that the primers were m164_Mut_rev and m164_SIINFEKA_for (5′-**AGTATAATCAACTTTGAAAAACTG**TTCTGGGCC GTCAACAACCAG-3′; nt 222,855 to 222,835), as well as m164_SIINFEKA_rev (5′-**CAGTTTTTCAAAGTTGATTATACT**GTCAGCGCCCCACGTCCGAC-3′; nt 222,883 to 222,902) and m164_Mut_for.

(ii) BAC mutagenesis. Mutagenesis of full-length mCMV bacterial artificial chromosome (BAC) plasmids pSM3fr (90) and pSM3fr-Δ*m06m152* (89) was performed in *Escherichia coli* strain DH10B (Invitrogen, Karlsruhe, Germany) by using a two-step replacement method (53, 58), with modifications described by Wagner et al. (90) and Borst et al. (6). Shuttle plasmid pST76K-m164_SIINFEKL was used to generate BAC plasmids pSM3fr-m164_SIINFEKL and pSM3fr-Δ*m06m152*-m164_SIINFEKL. Likewise, mutagenesis using shuttle plasmid pST76K-m164_SIINFEKA resulted in BAC plasmids pSM3fr-m164_SIINFEKA and pSM3fr-Δ*m06m152*-m164_SIINFEKA.

(iii) Reconstitution of BAC-derived recombinant viruses. The reconstitution of recombinant viruses by transfection of BAC plasmid DNA, as well as the routine elimination of BAC vector sequences, was performed in C57BL/6 primary mouse embryo fibroblasts (MEF) and verified by PCR as described previously (19, 79). Verified BAC-vector-free virus clones were used to prepare high-titer stocks of sucrose gradient-purified viruses (64) mCMV-m164_SIINFEKL (referred to as mCMV-SIINFEKL), mCMV-Δ*m06m152*-m164_SIINFEKL (mCMV-Δ*m06m152*-SIINFEKL), mCMV-m164_SIINFEKA (mCMV-SIINFEKA), and mCMV-Δ*m06m152*-m164_SIINFEKA (mCMV-Δ*m06m152*-SIINFEKA).

Cultivation and infection of cells. C57BL/6 MEF were prepared and cultivated as described previously (64). To enhance MHC-I cell surface expression and SIINFEKL peptide generation for antigen presentation analyses, IFN-γ pretreatment of MEF was performed for 48 h with 20 ng of IFN-γ per ml (R&D Systems, Wiesbaden, Germany). MEF were infected with wild-type (WT) BAC-derived mCMV MW97.03 (90), referred to here as mCMV-WT.BAC, or with the generated virus recombinants. Infection was performed with 0.2 PFU per cell under conditions of centrifugal enhancement of infectivity, which results in an effective multiplicity of infection (MOI) of 4 (41, 49; for details of the method, see reference 64).

Viral carrier protein expression. The expression of the authentic and mutated gp36.5/m164 proteins was monitored over the time course of infection of MEF in cell culture. The total protein content of infected MEF was isolated from cell lysates for subsequent Western blot analysis as described in greater detail previously (38).

CLSM analysis of viral carrier protein localization. Intracellular localization of authentic and mutated gp36.5/m164 proteins was examined by confocal laser scanning microscope (CLSM) immunofluorescence analysis (38). In brief, MEF were grown for 24 h on acetone-cleaned glass coverslips in 24-well plates at a density of $\sim 7 \times 10^4$ cells per coverslip. Centrifugal infection with mCMV was performed at an MOI of 4. At 8 h postinfection, MEF were washed with phosphate-buffered saline (PBS) and then fixed for 20 min at room temperature

with 4% (wt/vol) paraformaldehyde in PBS supplemented with 4% (wt/vol) sucrose. After fixation, cells were preincubated with blocking buffer (PBS supplemented with 0.3% [vol/vol] Triton X-100 and 15% [vol/vol] fetal calf serum [FCS]) for 30 min at room temperature. After this, 50 μl of blocking buffer containing an appropriate concentration of polyclonal affinity-purified rabbit antibodies directed against a C-terminal peptide of the gp36.5/m164 protein (34) was added to each coverslip, followed by overnight incubation in a humidity chamber. After five washes with PBS, each coverslip was incubated for 1 h with Alexa Fluor 546-conjugated goat anti-rabbit antibody (Invitrogen, Karlsruhe, Germany) diluted in blocking buffer. All incubations were performed at room temperature in the dark. After five further washes with PBS, cell nuclei were stained by incubation of the coverslips for 5 min with the DNA-binding blue fluorescent dye Hoechst 33342 (Invitrogen). Finally, cells were washed three times in PBS, and the coverslips were mounted in GelMount aqueous mounting medium (Sigma-Aldrich, Steinheim, Germany) for storage at 4°C in the dark. Immunofluorescence was examined using a Zeiss laser scanning microscope (LSM 510).

***In vivo* replicative fitness of viruses.** The *in vivo* replicative potential of BAC-cloned WT virus or virus mutants was determined by establishing virus growth curves for various host tissues of interest in the absence of immune control (79, 91). Specifically, C57BL/6 mice were immunocompromised by a 7-Gy total-body gamma irradiation performed at 24 h before intraplantar infection (64) with 10^5 PFU of the viruses under investigation. At defined times postinfection, virus replication in the spleen, lungs, and salivary glands was assessed by quantitation of infectivity present in the respective organ homogenates. The virus plaque assay (PFU assay) was performed with subconfluent third-passage MEF monolayers as permissive indicator cells by using the technique of centrifugal enhancement of infectivity as described in greater detail elsewhere (64). The number of infected cells in liver tissue sections was determined by immunohistochemistry (IHC) specific for the viral IE1 (pp89/76) protein, using the peroxidase-diaminobenzidine-nickel method for black staining of infected cell nuclei (64). Animal experiments were approved according to German federal law under permission number AZ 1.5 177-07-04/051-61.

Priming and quantitation of antiviral effector and memory CD8 T cells. Priming was accomplished by intraplantar infection of immunocompetent C57BL/6 mice with 10^5 PFU of the viruses under investigation. Acutely sensitized CD8 T cells and memory CD8 T cells were derived from pools of at least three spleens per group at 1 week and 35 weeks postinfection, respectively. The CD8 T cells were purified from splenocyte suspensions by positive immunomagnetic cell sorting as described previously (60). Frequencies of epitope-specific CD8 T cells were determined by an IFN-γ-based enzyme-linked immunospot (ELISPOT) assay as described in greater detail elsewhere (see reference 5 and references therein). In essence, graded cell numbers of responder CD8 T cells in triplicate assay cultures were incubated for 16 h with 10^5 peptide-loaded EL-4 (H-2^b) thymoma cells (per culture) as stimulator cells. Frequencies and their 95% confidence intervals were determined from the spot counts by intercept-free linear regression analysis, using the software Mathematica V6.0.1. Functional avidity of the epitope-specific CD8 T cells was assessed by using EL-4 stimulator cells loaded with antigenic peptides at $\log_{10}$-graded peptide concentrations.

Antigenic peptides and exogenous peptide loading. A list of the currently known mCMV-specific H-2^b class I (K^b and D^b)-restricted antigenic peptides is provided in a paper by Munks et al. (55). Custom peptide synthesis to a purity of >80% was performed by Jerini Peptide Technologies (Berlin, Germany). For exogenous peptide loading, EL-4 cells (in the ELISPOT assay [see above]) or IFN-γ-pretreated and infected or uninfected C57BL/6 MEF were incubated in cell suspension at defined concentrations of synthetic peptides for 1 h at ~22°C. Before use, excess unbound peptide was washed out.

Cytofluorometric analyses of K^b cell surface expression and presentation of K^b-SIINFEKL complexes. (i) Three-color cytofluorometric analysis. For measurement of the expression of total K^b and K^b-SIINFEKL complexes at the surfaces of infected C57BL/6 MEF, three-color staining was performed with phycoerythrin (PE)-conjugated mouse monoclonal antibody (MAb) anti-mouse H-$2K^b$ (2 μg/10^6 cells; Invitrogen), mouse MAb T-AG 25.D1-16 (65), specific for the K^b-SIINFEKL complex (1 μg/10^6 cells; eBioscience, San Diego, CA), and affinity-purified rabbit antibodies specific for the ER-resident mCMV glycoprotein gp36.5/m164 (see above; 0.2 μg/10^6 cells). All antibodies were pretested for their optimal concentration. Importantly, single and double staining of K^b and K^b-SIINFEKL gave comparable results, thus excluding any significant interference by competition for binding sites. For blocking of FcγIII/II receptors, MEF were preincubated with purified anti-mouse CD16/CD32 antibody (1 μg/10^6 cells; clone 2.4G2) (BD Biosciences). In the first step, cell surface staining was performed with MAb T-AG 25.D1-16 and with allophycocyanin (APC)-conjugated anti-mouse antibody (1 μg/10^6 cells; clone X56) (BD Biosciences) as the secondary antibody, followed by direct staining with the PE-conjugated anti-H-$2K^b$ antibody (see above). After treatment with BD Cytofix/Cytoperm Plus (BD Biosciences) to fix and permeabilize the cells, intracellular staining was accomplished with gp36.5/m164-specific rabbit antiserum antibodies and Alexa Fluor 488-conjugated anti-rabbit antibody (1 μg/10^6 cells; Invitrogen). Measurements were made with a Cytomics FC 500 cytofluorometer (Beckman Coulter, Fullerton, CA), using CXP Software 2.2. All viable cells were included in the analyses. Fluorescence intensities are displayed as logarithmic contour plots. Fluorescence channels FL-1, FL-2, and FL-4 represent Alexa Fluor 488, PE, and APC fluorescence, respectively.

(ii) Quantitation of cell surface antigens. For the absolute quantitation of total K^b molecules and K^b-SIINFEKL complexes at the surfaces of infected C57BL/6 MEF, a QIFIKIT (Dako, Glostrup, Denmark) kit was used according to the manufacturer's instructions. QIFIKIT allows a quantitative analysis of cell surface antigens by using standard bead populations with defined fluorochrome occupancies. These calibration beads are precoated with graded numbers of mouse monoclonal antibodies (mouse anti-human CD5; clone ST1) and are labeled prior to use with a saturating concentration of fluorescein isothiocyanate (FITC)-conjugated goat anti-mouse $F(ab)_2$ fragments provided in the kit, so that fluorescence correlates with the number of antibodies bound to the beads. The calibration beads were analyzed by flow cytometry, and the mean fluorescence intensity (MFI) of each bead population was recorded to establish a log-linear standard curve relating MFI (linear scale on the abscissa) to the number of bound antibodies (log scale on the ordinate), as illustrated in Fig. 6A. This standard curve can then be used to calculate the number of stained cell surface molecules by interpolation, as described in the manufacturer's protocol. To quantitate K^b molecules on the surfaces of infected C57BL/6 MEF as well as on uninfected C57BL/6 MEF present in the same cultures, a two-color cytofluorometric analysis was performed with mouse MAb anti-H-$2K^b$ (1 μg/10^6 cells; clone AF6-88.5) (BD Biosciences) labeled with FITC-conjugated goat anti-mouse $F(ab)_2$ fragments, combined with the intracellular staining of gp36.5/m164 as described above, except that Alexa Fluor 546-conjugated anti-rabbit antibody (1 μg/10^6 cells; Invitrogen) was used as secondary antibody. The FITC MFIs of $m164^+$ and $m164^-$ cell subsets were determined after respective electronic gating. The quantitation of K^b-SIINFEKL complexes, present on infected cells only, was performed accordingly by two-color cytofluorometric analysis after staining of K^b-SIINFEKL complexes with mouse MAb T-AG 25.D1-16 (1 μg/10^6 cells) labeled with FITC-conjugated goat anti-mouse $F(ab)_2$ fragments, combined with the intracellular staining of gp36.5/m164 and followed by electronic gating on $m164^+$ cells. Note that MAbs AF6-88.5 and T-AG 25.D1-16 were used at a saturating concentration to allow for absolute quantification of K^b and K^b-SIINFEKL, respectively.

Statistical analyses of significance. The statistical significance of differences between two independent sets of data was evaluated by using nonparametric, distribution-free tests, namely, the Wilcoxon-Mann-Whitney (rank sum) test for small sample sizes ($n < 10$) and the Kolmogorov-Smirnov test (KS test) for larger data sets, with at least 10 items in each data set. Online calculators are provided at http://elegans.swmed.edu/~leon/stats/utest.html (Ivo Dinov, Statistics Online Computational Resources, UCLA Statistics, Los Angeles, CA) and http://www.physics.csbsju.edu/stats (T. W. Kirkman), respectively. Data sets are considered to differ significantly if the P value is <0.05 (two sided).

RESULTS

Rationale for the approach of using SIINFEKL as a virally expressed reporter peptide for the quantitation of pMHC complexes presented at the cell surface. Cytofluorometric detection and quantitation of presented antigenic peptides require antibodies that are specific for the presentation complex, consisting of the peptide of interest bound to the restricting allelic form of MHC-I. Such antibodies are generally difficult to generate. Accordingly, only a few are described in the literature, none of which recognizes a presented CMV peptide (10, 12). The prototype of such an antibody is the MAb T-AG 25-D1-16, which recognizes the Ova-derived peptide SIINFEKL, presented by the MHC-I molecule K^b (65). In addition, OT-I mice express a transgenic TCR specific for the K^b-SIINFEKL complex (32). The availability of these tools has made SIINFEKL a widely used model system for immunological studies. To

exploit SIINFEKL for mCMV immunology in general, and here specifically for analyzing immunoevasin function in molecular terms, we generated BAC-cloned recombinant viruses mCMV-SIINFEKL and mCMV-Δ*m06m152*-SIINFEKL as well as the corresponding control viruses, in which a single amino acid substitution, L174A (codon CTG replaced with GCG), at the C-terminal MHC-I-binding anchor position of the peptide prevents its generation and presentation (Fig. 1). We employed such a strategy previously for the antigenic IE1 peptide of mCMV (79). We are not the first to have generated a recombinant mCMV that specifies SIINFEKL as a reporter peptide, but our concept differs in that mCMV-SIINFEKL, unlike the mCMV-Ova viruses (43, 80), does not ectopically express the foreign protein ovalbumin as the source for the peptide. Instead, the nonessential but abundantly synthesized viral protein gp36.5/m164, an ER-resident type I glycoprotein expressed in the early (E) phase of the viral replicative cycle, was used as a carrier protein in which the 9-codon sequence of the D^d-restricted immunodominant intrinsic peptide 167-AG PPRYSRI-175 (33, 35, 39) (amino acid positions are given relative to the start site of the primary translation product, p36) was replaced with the 8-codon sequence of SIINFEKL or, in the controls, SIINFEKA. This "orthotopic peptide swap" strategy, avoiding the expression of a foreign protein, was chosen with the intention to generate viruses not attenuated for *in vivo* growth. Figure 1A provides a genomic map of the peptide swap, and Fig. 1B shows sequencing data verifying the fidelity of the cloning procedures.

Integration of SIINFEKL does not alter expression or intracellular localization of the viral carrier protein. Although the approach was designed to keep alterations in the infected cells at the unavoidable minimum required for the intended immunological phenotype, and although gp36.5/m164 is not essential for virus replication, as revealed by the deletion mutant mCMV-Δ*m164* (data not shown), an impact of the integrated foreign sequence and of the deleted isoleucine at position 175 of the authentic protein needed to be ruled out. From previous studies characterizing the gp36.5/m164 protein, it was known that the antigenic sequence 167-AGPPRYSRI-175 is located in the luminal N-terminal region not affecting the transmembrane domain or the single N-glycosylation site (data not shown). Accordingly, its replacement with 167-SIINFEKL-174 in the recombinant carrier protein m164-SIINFEKL did not detectably reduce the apparent molecular mass and did not alter the E-phase kinetics of protein expression, with first detection by Western blot analysis 3 h after infection of permissive MEF (Fig. 2A). The recombinant carrier protein still localized to the ER (Fig. 2B). Thus, the peptide swap did not noticeably alter the basic properties of the protein.

Integration of SIINFEKL does not attenuate the virus for growth in relevant host tissues. Although expression kinetics and intracellular localization in infected MEF were unaltered, hidden differences in protein function might have an impact on virus replication. This needed to be ruled out. The SIINFEKL-expressing virus did not show an altered genome-to-infectivity ratio or deficient replication in multistep growth curve analysis in MEF cell cultures (data not shown). In different host organs, however, viruses are produced in diverse cell types (64), and infected cells are usually quiescent in the context of tissue. Accordingly, experience with other mCMV mutants, for instance, the Δ*ie1* mutant, shows that demonstration of unaltered virus growth in cultured fibroblasts does not necessarily exclude *in vivo* attenuation (20, 91). We therefore compared mCMV-WT.BAC and its derivative virus, mCMV-SIINFEKL, for growth in organs of immunocompromised C57BL/6 mice, including organs relevant for viral pathogenesis (spleen, lungs, and liver) and for horizontal virus transmission (salivary glands). Both viruses replicated comparably in the four organs tested (Fig. 3). Thus, insertion of SIINFEKL did not interfere with viral replicative fitness in the absence of an immune response.

Integration of SIINFEKL results in the intended immunological phenotype. The "orthotopic peptide swap" replacing an immunodominant intrinsic peptide with SIINFEKL was planned with the idea that the abundance of the carrier protein, its biochemical properties, and the peptide-flanking sequences should support efficient generation of the SIINFEKL peptide, or at least should not be adverse to it. The SIINFEKL epitope-specific immunogenicity of mCMV-SIINFEKL was revealed by priming of CD8 T cells in immunocompetent C57BL/6 mice (Fig. 4). Compared with a panel of intrinsic K^b- and D^b-restricted antigenic peptides (55), SIINFEKL proved to be intermediate in the epitope hierarchy with respect to the frequencies of responding *ex vivo* CD8 T cells in both the acute and the memory response (Fig. 4A, top panel). As intended, the point mutation L174A in gp36.5/m164 of mCMV-SIIN FEKA prevented the priming of SIINFEKL epitope-specific CD8 T cells (Fig. 4A, bottom panel), and stimulator cells loaded with peptide SIINFEKA were not recognized by CD8 T cells of mice primed with either of the two viruses, thus demonstrating the specificity of the response. As a side aspect, the data suggest that the L174A mutation facilitates the priming of CD8 T cells specific for the closely neighboring, intrinsic, D^b-restricted 176-WAVNNQAIV-184 peptide (55) (amino acid positions are given relative to the corrected start site of the primary translation product, p36). The reason for this might be more efficient processing of the downstream antigenic peptide precursor after removal of the N-terminally preceding proteasomal cleavage site, but this speculation was not further pursued here.

In accordance with previous findings with intrinsic mCMV epitopes (5, 21, 36, 56), enhanced antigen presentation by deletion of immunoevasin genes in mCMV-Δ*m06m152*-SIIN FEKL did not improve SIINFEKL-specific priming and did not alter the cumulative avidity distribution of the responding CD8 T cells (Fig. 4B). Rather, mCMV-SIINFEKL primed even more CD8 T cells, despite the inhibition of antigen presentation by the immunoevasins expressed in infected cells. This paradox was explained recently by enhanced virus replication and, thus, a sustained antigen supply for cross-priming by uninfected antigen-presenting cells in lymphoid tissues (5).

Endogenously generated K^b-SIINFEKL complexes reach the cell surface in detectable numbers only in the absence of immunoevasins. Cytofluorometric evaluation of the efficacy of immunoevasins was so far possible only for cell surface expression of all MHC-I molecules of a certain allele (34, 62, 89), not for mCMV-specific pMHC complexes. The conceptual difference is that measurement of total MHC-I steady-state levels includes molecules already present at the cell surface in advance of infection and loaded with "self" peptides, whereas

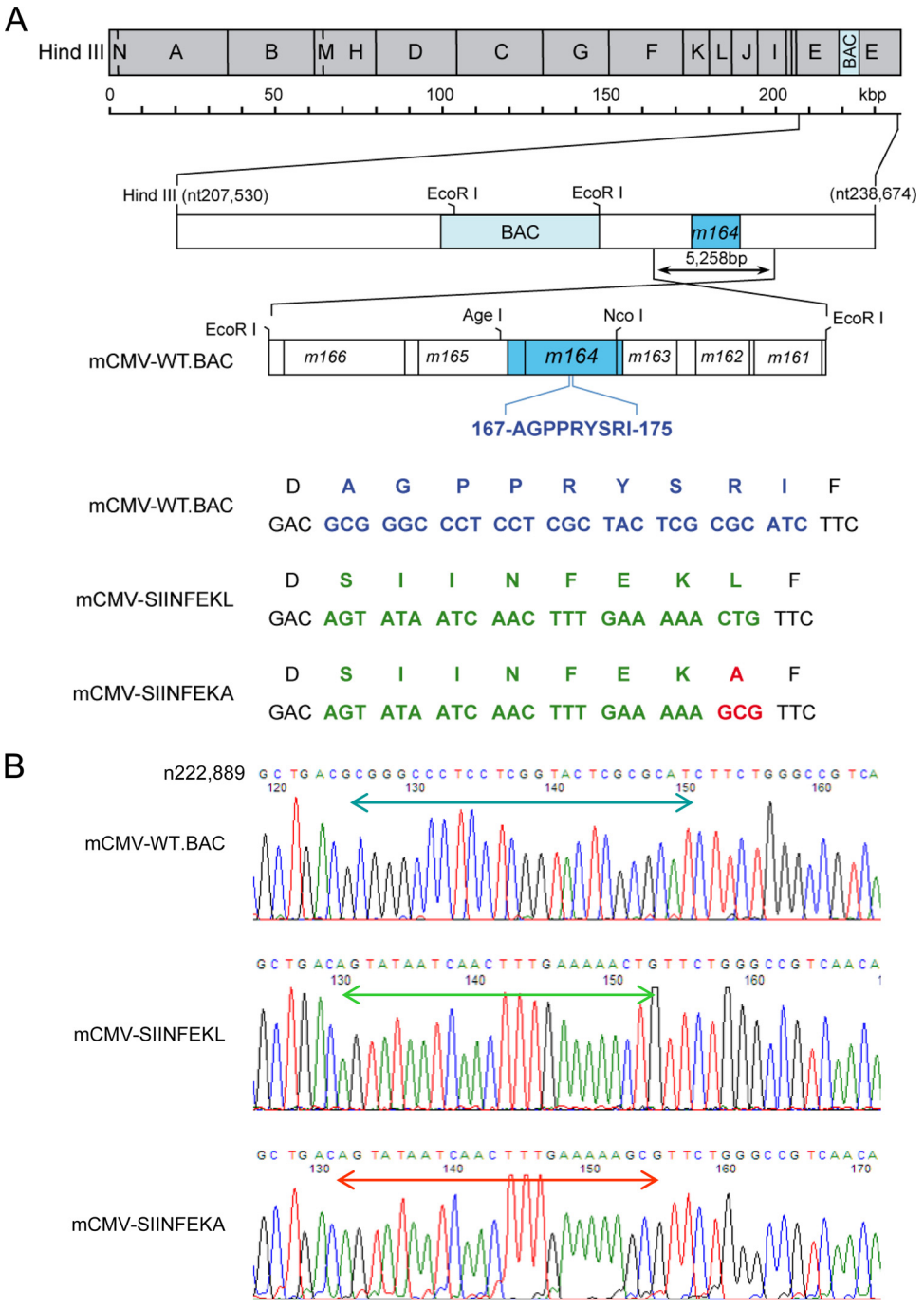

FIG. 1. Construction and sequencing of recombinant viruses with orthotopic peptide replacements. (A) Maps, drawn to scale, illustrating the mutagenesis design. The HindIII physical map of the mCMV BAC plasmid pSM3fr is shown at the top (53, 90), with the position of the BAC sequence within fragment E indicated by light blue shading. Note that this BAC sequence is cleaved out of the genome of the corresponding virus, mCMV-WT.BAC. The genomic region encompassing genes *m161* through *m166* is expanded to reveal the position of open reading frame (ORF) *m164*, which codes for the viral carrier protein gp36.5/m164, and its overlaps with neighboring ORFs (blue shading), as well as the map position of the peptide replacement site. Listed below are the amino acid sequences (including the N-terminal and C-terminal flanking residues) and the corresponding codons of the intrinsic antigenic peptide (dark blue lettering) and the peptides replacing it (green lettering), associated with deletion of isoleucine-175. The SIINFEKL C-terminal MHC anchor residue L174A mutation (codon CGC replaced with GCG instead of CTG) is highlighted in red. (B) Verification of the orthotopic peptide replacements by sequencing. Genomic regions encompassing the peptide-encoding codons were sequenced based on the recombinant BAC plasmids as well as on virion DNA. Shown here are the chromatograms of BAC plasmid sequencing. Signals from nucleotides A, T, G, and C are shown in green, red, black, and blue, respectively. Arrows span the sequences encoding the intrinsic antigenic peptide in mCMV-WT.BAC (blue), as well as the sequences encoding SIINFEKL (green) and SIINFEKA (red) in the peptide swap mutants mCMV-SIINFEKL and mCMV-SIINFEKA, respectively. Analogous mutations were introduced into a BAC plasmid that lacks the immune evasion genes *m06* and *m152* (89) and were verified accordingly by sequencing.

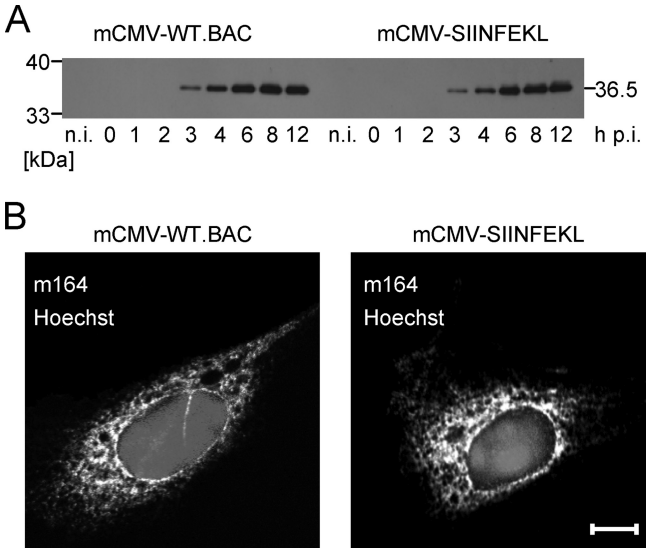

FIG. 2. Molecular integrity of recombinant protein m164-SIINFEKL expressed by mCMV-SIINFEKL. (A) Protein expression kinetics. The Western blot shows the apparent molecular mass and E-phase expression of the authentic (left portion of the blot) and mutated (right portion of the blot) m164 glycoproteins after infection of C57BL/6 MEF at an MOI of 4 with viruses mCMV-WT.BAC and mCMV-SIINFEKL, respectively. h p.i., hours postinfection. (B) Unaltered intracellular distribution of recombinant protein m164-SIINFEKL. Shown are confocal laser scanning images revealing the cytoplasmic (ER) distribution of authentic and mutated m164 glycoproteins (Alexa Fluor 546 fluorescence) 8.5 h after infection of MEF (see above) with viruses mCMV-WT.BAC (left) and mCMV-SIINFEKL (right). Nuclear DNA was stained with Hoechst 33342 dye. Bar, 10 μm. Corresponding data were obtained for mCMV-SIINFEKA (data not shown).

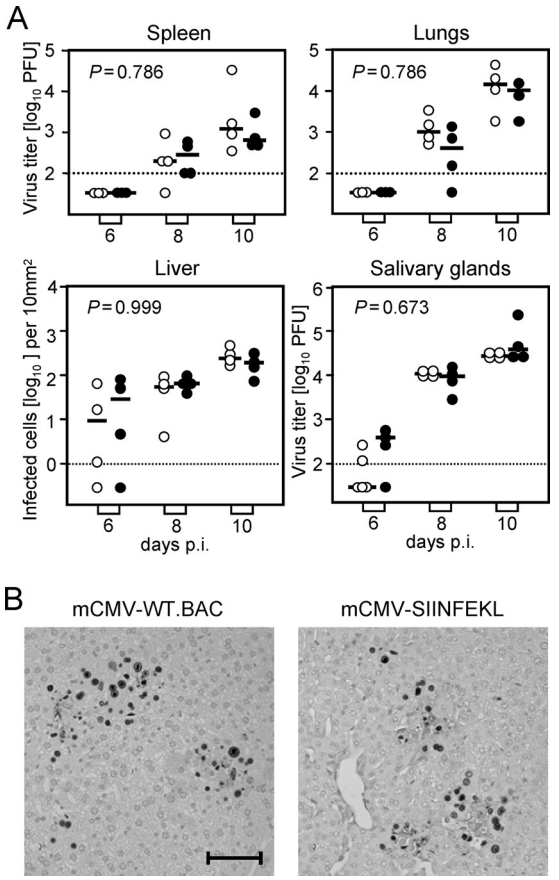

FIG. 3. Orthotopic peptide swap in the gp36.5/m164 carrier protein does not interfere with viral replicative fitness in host organs. (A) The recombinant virus mCMV-SIINFEKL is not attenuated for growth *in vivo*. Shown are virus growth curves for the indicated organs of immunocompromised C57BL/6 mice. Symbols represent virus titers (PFU per organ) in the case of the spleen, lungs, and salivary glands, as well as numbers of infected cells, mostly hepatocytes, in representative 10-mm^2 areas of liver tissue sections for individual mice. Median values are indicated by short horizontal bars. Empty circles, mCMV-WT.BAC; filled circles, mCMV-SIINFEKL. The dotted lines represent the detection limits of the respective assays. p.i., postinfection. The indicated *P* values were calculated by the nonparametric, distribution-free Kolmogorov-Smirnov test for comparison of two data sets. The empirical distribution functions for the two data sets are considered significantly different for *P* values of <0.05, which was not the case for any of the organs tested. (B) Unaltered viral histopathology in the liver. The images show the immunohistological analysis of virus spread in the liver on day 10 after infection with mCMV-WT.BAC (left) and mCMV-SIINFEKL (right). Foci of infected liver cells are visualized by black staining of the intranuclear IE1 protein pp89/76. Bar, 50 μm. Corresponding data were obtained for mCMV-SIINFEKA (data not shown).

specific pMHC complexes more directly reveal the fate of MHC-I molecules recently loaded with processed peptides derived from viral proteins. Since both immunoevasins and the recombinant carrier protein m164-SIINFEKL are expressed in the E phase, SIINFEKL does not have an advantage by expression kinetics, and therefore immunoevasins are expected to block its presentation efficiently.

Three-color cytofluorometric analysis was performed to correlate the expression of K^b, K^b-SIINFEKL, and the carrier protein gp36.5/m164 16 h after infection of C57BL/6 MEF with the mCMV-SIINFEKL and mCMV-Δ*m06m152*-SIINFEKL viruses (Fig. 5). It is obvious that K^b-SIINFEKL must be absent from m164$^-$ cells not expressing the recombinant carrier protein. It is important that in our experience, not all MEF are productively infected in cultures, even if the multiplicity of infection statistically predicts that all cells should be hit by infectious virus (34). Although originally not intended, this phenomenon provides us with a useful intrinsic standard for MHC-I expression by uninfected cells present in the cytokine milieu of an infected cell culture. The presence of uninfected cells also makes evident, however, that distinction between infected and uninfected cells by use of an infection marker is crucial in these studies.

Infection of the MEF cultures with mCMV-SIINFEKL resulted in three MEF subsets defined by cell surface expression of the MHC-I molecule K^b, namely, uninfected cells with high expression of K^b (m164$^-$ $K^{b\ high}$) as well as infected cells with intermediate (m164$^+$ $K^{b\ intermediate}$) and low (m164$^+$ $K^{b\ low}$) expression of K^b (Fig. 5a). In contrast, infected cells displayed no detectable K^b-SIINFEKL complexes at the cell surface compared with the uninfected cells of the same cultures (Fig. 5c), although K^b-SIINFEKL complexes were present inside the infected cells (CLSM analysis [data not shown]). The explanation that low expression of K^b and K^b-SIINFEKL results from the function of immunoevasins is supported by their

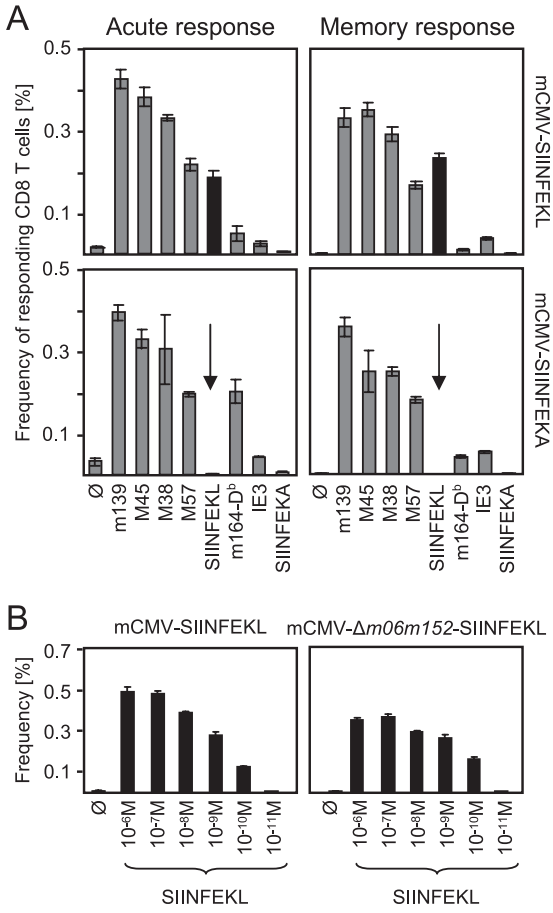

FIG. 4. Immunogenicity phenotype of mCMV-SIINFEKL. (A) Rank of SIINFEKL in the immunodominance hierarchy of H-2^b-restricted mCMV peptides. Intraplantar infection of immunocompetent C57BL/6 mice was performed with 10^5 PFU of mCMV-SIINFEKL (upper panels) and mCMV-SIINFEKA (lower panels). Frequencies of peptide-specific CD8 T cells in the spleen were determined for pools of three mice per group during the acute immune response 1 week after priming (left panels) and during immunological memory in latently infected mice after 35 weeks (right panels). The ELISPOT assay was performed with immunomagnetically purified CD8 T cells as responder cells and with EL-4 stimulator cells exogenously loaded with saturating concentrations of synthetic antigenic peptides corresponding to the H-2^b-restricted epitopes indicated. Gray (for intrinsic antigenic peptides) and black (for SIINFEKL) columns represent the frequencies of responding CD8 T cells, and error bars indicate the 95% confidence intervals determined by intercept-free linear regression analysis. Arrows highlight the absence of SIINFEKL-specific CD8 T cells after infection with mCMV-SIINFEKA, which shows the epitope specificity of priming. Ø, EL-4 cells with no viral peptide added. (B) Impact of immunoevasins on functional avidities of SIIN FEKL-specific CD8 T cells. Cumulative avidity distributions were determined by measuring the frequencies of SIINFEKL-specific CD8 T cells capable of responding in the ELISPOT assay to EL-4 stimulator cells exogenously loaded with synthetic SIINFEKL peptide at the $\log_{10}$-graded peptide concentrations indicated. Responder CD8 T cells were derived by immunomagnetic cell sorting from splenocytes (pool of three donor spleens per group) on day 7 after intraplantar infection with 10^5 PFU of the viruses mCMV-SIINFEKL (left panel) and mCMV-Δ*m06m152*-SIINFEKL (right panel). Frequencies (black columns) and the corresponding upper 95% confidence limits (error bars) were calculated by intercept-free log-linear regression analysis. Ø, EL-4 cells with no peptide added.

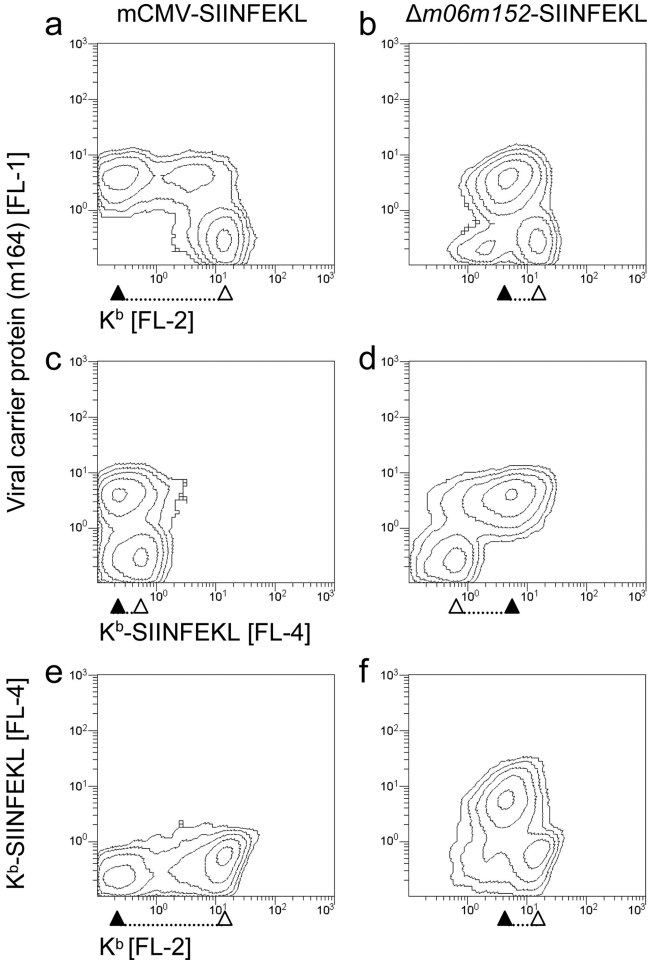

FIG. 5. Regulation of K^b and K^b-SIINFEKL cell surface presentation by immunoevasins. For endogenous antigen processing and presentation in the presence or absence of immunoevasins, IFN-γ-pretreated C57BL/6 MEF were infected at an MOI of 4 (centrifugal infection corresponding to 0.2 PFU per cell) with viruses mCMV-SIINFEKL (panels a, c, and e) and mCMV-Δ*m06m152*-SIINFEKL (panels b, d, and f). Three-color cytofluorometric analyses were performed after 16 h, that is, at an advanced stage of the E phase of viral gene expression. Logarithmic contour plots reveal fluorescence intensity levels for ~35,000 live cells analyzed, with no further gating. For panels a to d, ordinate fluorescence data (FL-1; Alexa Fluor 488) represent expression of the viral cytoplasmic E-phase protein gp36.5/m164, which serves as the carrier protein for SIINFEKL, and abscissa fluorescence data represent cell surface expression of the MHC-I molecule K^b (a and b) (FL-2; PE) and the pMHC complex K^b-SIINFEKL (c and d) (FL-4; APC). Panels e and f relate the expression of K^b-SIINFEKL (ordinate; FL-4) to the expression of K^b (abscissa; FL-2). Caliper rules highlight the effect of immunoevasins by showing the differences in the abscissa fluorescence modal values between infected $m164^+$ cells (filled arrowheads) and uninfected $m164^-$ cells (empty arrowheads) present in the same cultures.

elevated expression at the surfaces of cells infected with the immunoevasin gene deletion mutant mCMV-Δ*m06m152*-SIINFEKL (compare Fig. 5b and d with Fig. 5a and c, respectively). Notably, however, even in the absence of these two immunoevasins, expression of K^b in infected cells did not reach the level of expression found in uninfected cells. This finding suggests the involvement of an additional infection-associated

parameter that reduces cell surface MHC-I expression relative to that of uninfected cells. This is certainly not the third vRAP gp34/m04, since an analogous finding was made previously for the expression of MHC-I L^d in BALB/c MEF infected with an mCMV mutant in which all three vRAP genes were deleted (34). Interestingly, the expression of K^b in the absence of immunoevasins was similar to the expression in the $m164^+$ $K^{b\ intermediate}$ subset seen after infection with mCMV-SIINFEKL (Fig. 5a and b), suggesting that this is a subpopulation of infected cells in which immunoevasins have not yet completed MHC-I downmodulation at the time of analysis. We have no immediate explanation for the occurrence of an uninfected cell population with low K^b expression in cultures infected with the deletion mutant (Fig. 5b), but this phenomenon was reproduced in the independent experiment shown in Fig. 7 (see panels b and d). It is interesting that cell surface expression of K^b-SIINFEKL complexes in infected cells was not proportional to the cell surface expression of total K^b (Fig. 5e and f), which is likely explained by the presence of many unrelated pMHC complexes at the cell surface.

In conclusion, as known from previous work (34, 62, 89), mCMV immunoevasins eventually downmodulate the steady-state level of MHC-I at the cell surface. The new information revealed here by detection of K^b-SIINFEKL is that the presentation of recently generated pMHC complexes is affected more completely and is obviously much faster.

Molecular quantitation of K^b and K^b-SIINFEKL cell surface presentation depending on immunoevasins. Previous work has documented the qualitative effect of mCMV immunoevasins on epitope presentation to CD8 T cells (34, 62). Sensitization of CD8 T cells to effector functions such as cytolytic activity or cytokine release occurs through recognition of pMHC complexes by the TCR. This is an on-or-off event that depends on a variable threshold of epitope presentation required for triggering, a threshold that is defined by TCR affinities of the particular epitope-specific polyclonal or clonal CD8 T-cell populations used for the analysis. Thus, quantitative differences in antigen presentation above the sensitization threshold of the respective responder CD8 T-cell population cannot be resolved, and the impact of immunoevasins cannot be expressed in terms of absolute differences in the numbers of pMHC complexes displayed at the cell surface. This problem is solved by using TCR-mimicking antibodies specific for pMHC complexes, specifically MAb T-AG 25.D1-16, recognizing K^b-SIINFEKL (65), in this case. Likewise, the total number of K^b molecules is determined with a MAb specific for K^b (Fig. 6).

Using calibration beads with graded fluorochrome binding capacities, a standard curve was established to relate mean fluorescence intensity to the number of bound antibodies (Fig. 6A, top). With this assay, the average number of K^b molecules displayed on the surfaces of uninfected cells present in infected cell cultures (Fig. 5) was determined to be in the range of 3×10^5 per cell, whereas cells infected with mCMV-SIINFEKL displayed only 4×10^4 K^b molecules. This difference is explained only in part by the expression of immunoevasins, since infection with mCMV-Δ*m06m152*-SIINFEKL reduced K^b expression to 1.5×10^5 molecules per cell. Thus, in this selected example, immunoevasins accounted for a reduction of ~4-fold within 16 h of infection (Fig. 6A, center). Presentation of K^b-SIINFEKL was found to be on the order of 1.5×10^4 complexes per cell after infection with mCMV-Δ*m06m152*-SIINFEKL, which corresponds to a K^b occupancy by SIINFEKL of 10% in the absence of immunoevasins. The absolute number was reduced in this specific experiment, to below the detection limit of 100 K^b-SIINFEKL complexes, in the presence of immunoevasins in cells infected with mCMV-SIINFEKL (Fig. 6A, bottom).

Figure 6B compiles the results of all our quantitation experiments to show epitope specificity, reproducibility, variance, and significance of differences. First of all, staining with MAb T-AG 25-D1-16 did not give any quantifiable fluorescence signals with uninfected cells or cells infected with SIINFEKA-expressing viruses. These important negative controls thus showed that T-AG 25-D1-16 does not noticeably cross-react with potentially "mimotopic" complexes (11, 81) formed between K^b or D^b molecules and any of the many intrinsic cellular or mCMV-encoded antigenic peptides or with any other cellular or viral cell surface proteins.

Regarding the cell surface expression of K^b in infected cells, the reduction by immunoevasins was ~3-fold within 16 h, based on the median values (combined for SIINFEKA- and SIINFEKL-expressing viruses) of 1×10^5 and 3×10^4 between viruses lacking and expressing immunoevasins, respectively, with no significant difference between SIINFEKA- and SIINFEKL-expressing viruses. In contrast, immunoevasins reduced cell surface presentation of K^b-SIINFEKL complexes by a factor of ~50, based on the median values of 1×10^4 and 200 after infection with mCMV-Δ*m06m152*-SIINFEKL and mCMV-SIINFEKL, respectively. Thus, in relative terms, referred to the data at 16 h postinfection, the effect of immunoevasins on the cell surface expression of K^b-SIINFEKL complexes was about 15-fold stronger than that on the cell surface expression of all K^b molecules.

Formation of pMHC complexes by exogenous peptide loading is proportional to the cell surface density of MHC-I molecules. Unlike the situation found after endogenous generation of pMHC complexes as a result of antigen processing, where cell surface expression of K^b-SIINFEKL and total K^b did not correlate (Fig. 5e and f), binding of synthetic antigenic peptides as exogenous ligands should be proportional to the number of MHC-I molecules available as receptors at the cell surface. Accordingly, the effect of immunoevasins on K^b steady-state levels, as described above for SIINFEKL-expressing viruses (Fig. 5a and b), should be paralleled by their effect on exogenous peptide loading. To verify this prediction experimentally, C57BL/6 MEF were infected with viruses mCMV-SIINFEKA and mCMV-Δ*m06m152*-SIINFEKA, both lacking endogenous presentation of SIINFEKL, followed 16 h later by incubation with a high concentration (10^{-4} M) of synthetic SIINFEKL peptide (Fig. 7A). The overall expression of K^b reproduced the findings obtained with the corresponding SIINFEKL-expressing viruses (compare Fig. 5 and 7A, panels a and b). As expected, uninfected $m164^-$ cells present in the infected cultures now all displayed K^b-SIINFEKL, whereas the absence and presence of K^b-SIINFEKL on infected $m164^+$ cells reflected the presence and absence of immunoevasins, respectively (Fig. 7A, panels c and d). In accordance with the theory, cell surface display of K^b-SIINFEKL complexes turned out to be directly proportional to the expression of K^b (Fig. 7A, panels e and f), a finding which also implies that the two

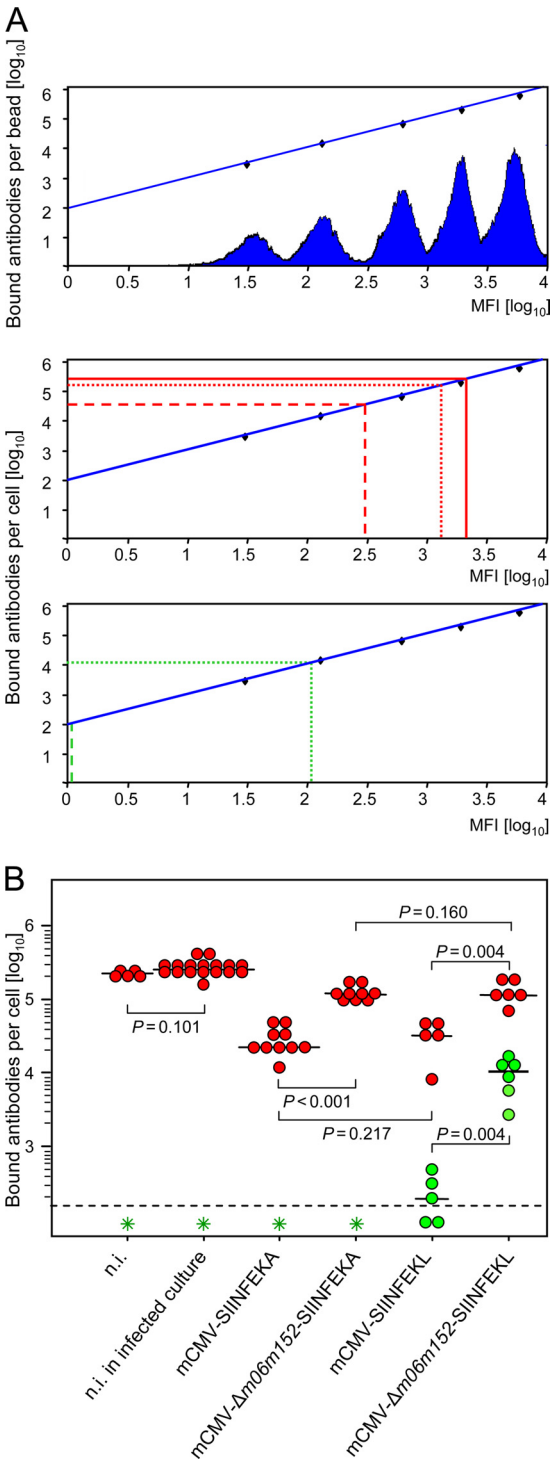

FIG. 6. Molecular quantitation of K^b and K^b-SIINFEKL cell surface presentation dependent upon the expression of immunoevasins. (A) Documentation of the cytofluorometric quantification procedure. Throughout, centrifugal infections of IFN-γ-pretreated C57BL/6 MEF were performed to result in an MOI of 4, and cell surface expression was determined 16 h after infection. (Top) Standard curve relating MFI values in channel FL-1 (FITC) to numbers of bound antibodies, using a QIFIKIT calibration kit. For illustration, the corresponding fluorescence histograms (the ordinate scale for the number of events is not depicted) for the calibration bead populations are displayed. (Center) Quantitation of total cell surface K^b on uninfected cells present in infected cell cultures (solid red line), on cells infected with mCMV-SIINFEKL (dashed red line), and on cells infected with mCMV-Δ*m06m152*-SIINFEKL (dotted red line). (Bottom) Quantitation of cell surface K^b-SIINFEKL complexes on cells infected with mCMV-SIINFEKL (dashed green line) and mCMV-Δ*m06m152*-SIINFEKL (dotted green line). (B) Compilation of quantitation results from several independent experiments showing the statistical significance of immunoevasin function. Viruses used for infection are indicated. Controls included IFN-γ-pretreated uninfected MEF (n.i. [not infected]) as well as uninfected cells present in infected cell cultures (n.i. in infected culture). Red and green circles represent quantitations of cell surface K^b and K^b-SIINFEKL complexes, respectively. Median values for data from independent experiments are marked by short horizontal bars. The dashed line represents the detection limit of the assay. Green asterisks indicate the absence of signals for K^b-SIINFEKL complexes, which shows that MAb T-AG 25.D1-16 does not cross-react with anything else in uninfected or mCMV-infected cells not expressing SIINFEKL. *P* values calculated with the distribution-free Wilcoxon-Mann-Whitney rank-sum test are indicated for group comparisons of major interest. Differences are regarded as significant for *P* value of <0.05 (two sided).

antibodies do not interfere with each other in binding to K^b-SIINFEKL complexes.

For quantitating exogenous K^b loading capacity depending upon infection with SIINFEKA-expressing viruses in the absence or presence of immunoevasins, we determined the proportion of SIINFEKL-presenting K^b molecules among all cell surface K^b molecules, that is, the K^b occupancy by SIINFEKL, as a function of the SIINFEKL peptide concentration (Fig. 7B). Uninfected cells present in cultures infected with mCMV-SIINFEKA or mCMV-Δ*m06m152*-SIINFEKA served as a positive reference that revealed a K^b occupancy of ~6.5% after incubation with 10^{-4} M synthetic SIINFEKL peptide, rapidly declining at lower peptide concentrations. Thus, even with uninfected cells, replacement of intrinsically presented peptides requires a high concentration of an exogenously provided competitor peptide. As expected, the type of infecting virus did not matter for uninfected cells in the cultures. Notably, with the sensitivity of the assay, K^b-SIINFEKL complexes were barely detectable on cells infected with mCMV-SIINFEKA, despite the high SIINFEKL peptide loading concentration of 10^{-4} M, and deletion of immunoevasins improved the K^b occupancy by exogenously supplied SIINFEKL to only ~1%. Thus, though immunoevasins do play a role, additional parameters associated with infection must be involved in determining MHC-I occupancy after exogenous peptide loading.

Immunoevasins preferentially target the cell surface transport of recently generated pMHC complexes. A possible explanation for the differential effect of immunoevasins on K^b-SIINFEKL complexes and total cell surface K^b could be that immunoevasins inhibit the transport of K^b-SIINFEKL to the cell surface more efficiently than the transport of other K^b-peptide complexes. We considered it a more likely mechanism, however, that K^b-peptide complexes present at the cell surface in advance of infection were less affected by immunoevasins than recently generated, peptide-loaded K^b molecules traveling from the ER to the cell surface. To test this hypothesis, cells were incubated with a high dose of exogenously supplied synthetic SIINFEKL peptide (10^{-4} M) (Fig. 7B) prior to the expression of immunoevasins immediately after infection

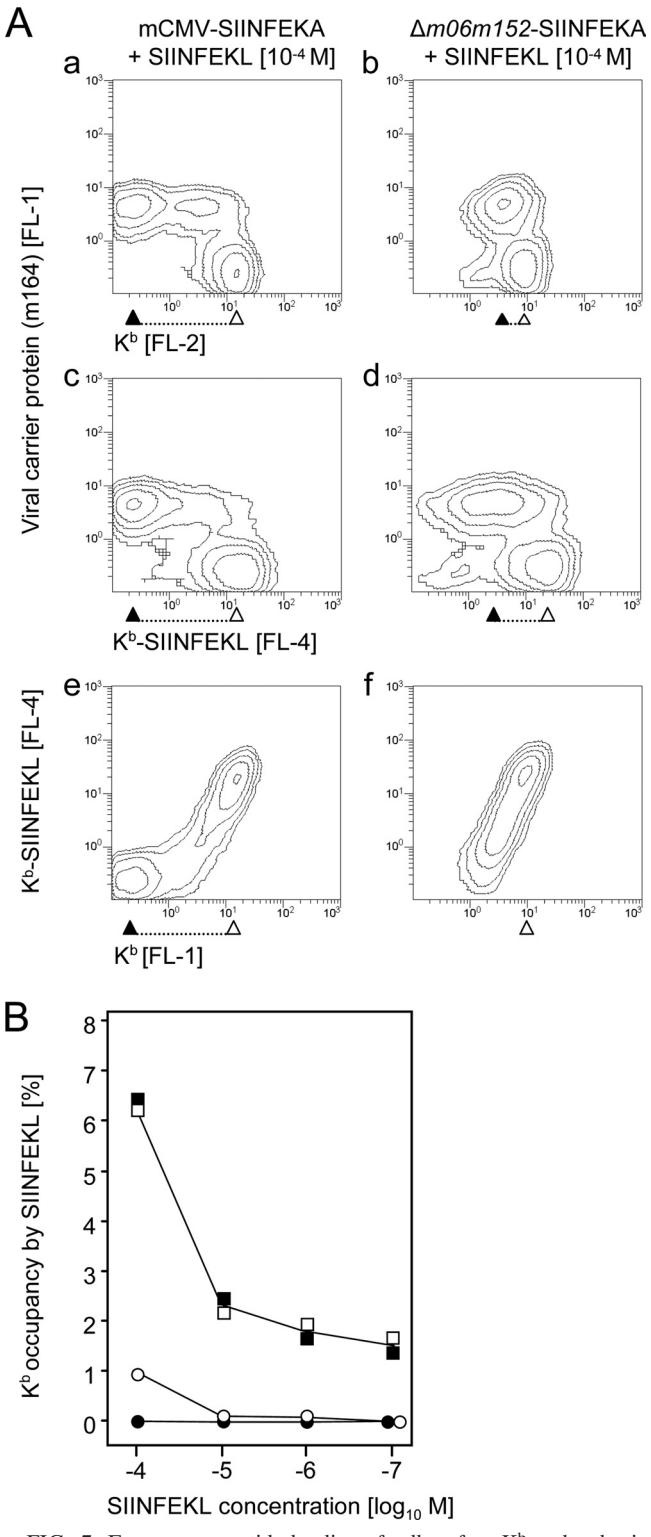

FIG. 7. Exogenous peptide loading of cell surface K^b molecules is strongly reduced by preceding expression of immunoevasins. (A) Exogenous peptide loading is proportional to the number of cell surface MHC-I molecules. To analyze selectively the cell surface "loadability" of infected cells with exogenously supplied SIINFEKL peptide, endogenous processing and presentation of SIINFEKL were avoided by infecting IFN-γ-pretreated C57BL/6 MEF at an MOI of 4 with viruses mCMV-SIINFEKA (a, c, and e) and mCMV-Δ*m06m152*-SIINFEKA (b, d, and f). Infection was allowed to proceed for 16 h, to a late stage of the E phase, shortly prior to viral DNA replication, so that immunoevasins could fully exert their effects on K^b cell surface expression. Exogenous loading of K^b molecules for the generation of K^b-SIINFEKL complexes was then accomplished by incubating the infected cells with synthetic SIINFEKL peptide at a concentration of 10^{-4} M. Shown are logarithmic contour plots of three-color cytofluorometric analyses of ~35,000 live cells, relating the cytoplasmic expression of the carrier protein gp36.5/m164 to the cell surface expression of K^b (a and b) and K^b-SIINFEKL (c and d), as well as correlating K^b and K^b-SIINFEKL expression (e and f). Cytofluorometric labels were as specified in the legend to Fig. 5. Caliper rules highlight the effect of immunoevasins by showing the differences in the abscissa fluorescence modal values between infected $m164^+$ cells (filled arrowheads) and uninfected $m164^-$ cells (empty arrowheads) present in the same cultures. (B) Occupancy of cell surface K^b molecules by SIINFEKL depending on the loading peptide concentration. Cells were infected, as specified above, and 16 h later the infected cells were incubated with $\log_{10}$-graded concentrations of synthetic SIINFEKL peptide (abscissa). Cell surface K^b molecules and K^b-SIINFEKL complexes were quantitated as outlined in greater detail in the legend to Fig. 6, and the proportion of SIINFEKL-loaded K^b molecules was calculated (ordinate). Filled and empty circles represent cells infected with mCMV-SIINFEKA and mCMV-Δ*m06m152*-SIINFEKA, respectively. Filled and empty squares represent uninfected cells present in cultures infected with mCMV-SIINFEKA and mCMV-Δ*m06m152*-SIINFEKA, respectively.

with mCMV-SIINFEKA or, for comparison, with mCMV-Δ*m06m152*-SIINFEKA, so that the fate of preloaded K^b-SIINFEKL could be studied selectively in the absence of endogenously replenished K^b-SIINFEKL (Fig. 8). To limit the loss of cell surface K^b-SIINFEKL complexes due to the constitutive MHC-I turnover (15, 52; for a review, see reference 13) independent of a direct immunoevasin function, measurements were now performed 8 h after infection instead of 16 h after infection as in the preceding experiments. Though this is an early time in the viral replication cycle, the epitope-carrying protein gp36.5/m164 and the immunoevasins, all of which are E-phase proteins, should still have enough time to play their roles.

As shown by cytofluorometric analysis, preloaded K^b-SIINFEKL complexes at the cell surface were only moderately affected by immunoevasins 8 h after infection with mCMV-SIINFEKA in comparison to infection with mCMV-Δ*m06m152*-SIINFEKA (Fig. 8A, panels a and b). In contrast to this, an 8-h period indeed proved to be sufficient for endogenous presentation of K^b-SIINFEKL after infection of peptide-unloaded MEF with mCMV-Δ*m06m152*-SIINFEKL, as well as for prevention of its presentation by immunoevasins after infection with mCMV-SIINFEKL (panels d and c, respectively). The corresponding analysis of total K^b cell surface expression by these cells (panels a* through d*) revealed a fate of cell surface-resident K^b molecules comparable to that of exogenously loaded K^b-SIINFEKL complexes, namely, an only moderate reduction during 8 h of infection in the presence of immunoevasins. These findings were further substantiated by quantitation of cell surface K^b-SIINFEKL complexes combined with statistical analysis of compiled experiments showing reproducibility, variance, and statistical significance (Fig. 8B). Exogenous loading with SIINFEKL peptide immediately following infection with mCMV-Δ*m06m152*-SIINFEKA defined the reference level of K^b-SIINFEKL presentation reached at

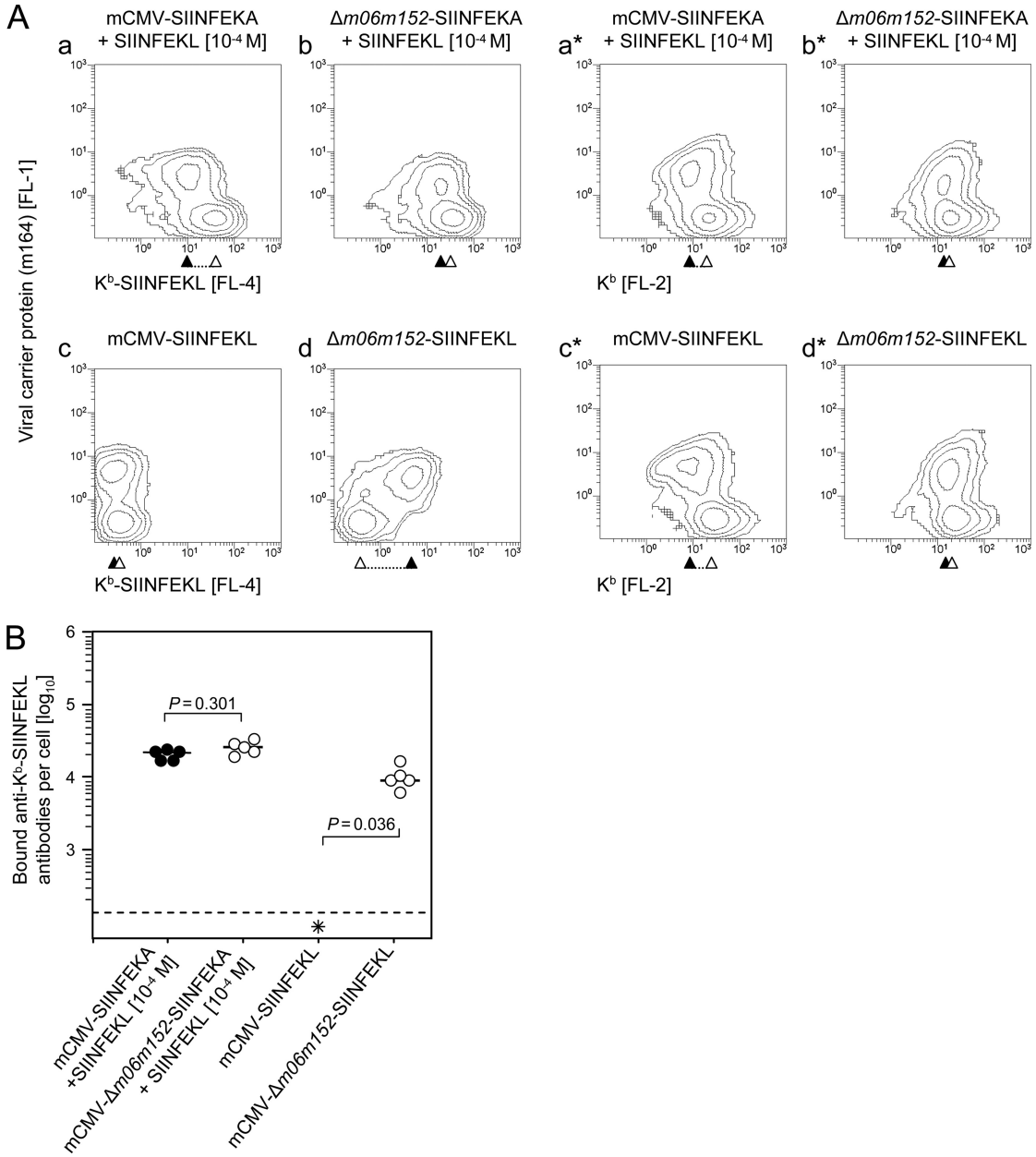

FIG. 8. Immunoevasins only slowly downmodulate preexisting cell surface K^b-peptide complexes. (A) Effect of immunoevasins on K^b-SIINFEKL complexes and on all K^b molecules present at the cell surface in advance of immunoevasin gene expression. K^b molecules on the surfaces of IFN-γ-pretreated C57BL/6 MEF were pulse labeled by exogenous loading with synthetic SIINFEKL peptide at a concentration of 10^{-4} M immediately after their infection with viruses mCMV-SIINFEKA and mCMV-Δ*m06m152*-SIINFEKA (panels a and a∗ and panels b and b∗, respectively). It is important that this sequence of "infection first and peptide loading thereafter" was chosen in order to avoid a possible interference of peptide loading with the adhesion and penetration of the infecting viruses, but the peptide loading clearly preceded the expression of the immunoevasin genes in the E phase. A further, more technical reason was that centrifugal infection requires adherent cells, whereas peptide loading is more efficient with cells in suspension. For comparison, endogenous peptide loading was accomplished by infection of cells with viruses mCMV-SIINFEKL and mCMV-Δ*m06m152*-SIINFEKL (panels c and c∗ and panels d and d∗, respectively). Three-color cytofluorometric analysis relating the cytoplasmic expression of the viral E-phase protein gp36.5/m164 (ordinate) to the cell surface expression of K^b-SIINFEKL complexes and total K^b (abscissas in panels a to d and panels a∗ to d∗, respectively) was performed 8 h after infection. For labeling information, see the legend to Fig. 5. The plots displayed are logarithmic contour plots representing fluorescence intensity levels for ~35,000 live cells analyzed, with no further gating. Caliper rules highlight the effect of immunoevasins by showing the differences in the abscissa fluorescence modal values between infected $m164^+$ cells (filled arrowheads) and uninfected $m164^-$ cells (empty arrowheads) present in the same cultures. (B) Compilation of quantitation results from five independent experiments (filled or empty circles) demonstrating a significant effect of immunoevasins on endogenously loaded but not exogenously preloaded K^b-SIINFEKL complexes. The quantitation of K^b-SIINFEKL complexes on the surfaces of cells was performed as outlined in greater detail in the legend to Fig. 6. Protocols for infection and peptide loading are indicated. Filled circles and empty circles represent the presence and absence of immunoevasins, respectively. Median values are marked by short horizontal bars. The asterisk indicates the absence of signals for quantitation. *P* values calculated with the distribution-free Wilcoxon-Mann-Whitney rank-sum test are indicated for group comparisons of major interest. Differences are regarded as significant for *P* values of <0.05 (two sided).

the time of analysis due to constitutive MHC-I turnover and also accounted for a possible influence of parameters of infection other than immunoevasins. Notably, further reduction mediated by the expression of immunoevasins after infection with mCMV-SIINFEKA did not reach statistical significance at 8 h postinfection ($P = 0.301$), whereas at the same time, blockade of endogenous presentation of SIINFEKL after infection of peptide-unloaded MEF with mCMV-SIINFEKL was significant, both numerically (10^4 complexes reduced to below the detection limit) and statistically ($P = 0.036$).

Altogether, these data provide strong evidence to suggest that immunoevasins function mainly by inhibiting the transport of recently generated pMHC complexes to the cell surface, whereas a decline in total cell surface MHC-I molecules is time dependent and secondary to turnover in the absence of replenishment.

DISCUSSION

Comparative quantitation of the total MHC-I molecules of a given allele at the cell surface and of a defined antigenic peptide presented by the same allelic form of MHC-I, the K^b-SIINFEKL complex in this case, gave us for the first time an impression of the quantitative changes at the cell surface that are effected by the combined action of mCMV immunoevasins gp48/m06 and gp40/m152. This progress in knowledge was made possible by versatile novel tools introduced with this study, namely, viruses mCMV-SIINFEKL and mCMV-Δ*m06m152*-SIINFEKL, expressing the K^b-restricted reporter peptide SIINFEKL in the presence and absence of mCMV immunoevasins, respectively. It is important that the reporter peptide was expressed by an "orthotopic peptide swap" in place of an immunodominant D^d-restricted peptide of the viral E-phase glycoprotein gp36.5/m164. It thus behaves like a viral peptide and is expressed according to the regular gene expression kinetics of its viral carrier protein. It is therefore expected that antigen presentation data obtained with these viruses reflect the physiological situation much more closely than do data obtained with transfection-based or vector-based protein overexpression systems or after ectopic expression of foreign proteins in mCMV. Specifically, in the related SIINFEKL expression system of infection with mCMV-Ova, the foreign protein ovalbumin is expressed with immediate-early kinetics under the control of the human CMV major immediate-early promoter-enhancer (80), so its synthesis and antigen processing precede the function of the immunoevasins gp48/m06 and gp40/m152, both of which are expressed in the E phase. Since most mCMV epitopes are actually derived from E-phase proteins (33, 55), SIINFEKL processed from an E-phase carrier protein should be a reliable reporter for immunoevasin function.

Notably, SIINFEKL can be employed to serve a dual reporter function. While endogenously processed SIINFEKL is used to follow the fate of an antigenic viral peptide after infection, exogenously loaded SIINFEKL replacing cellular "self" peptides can report the fate of peptides that are presented in advance of infection, provided that a fresh supply of SIINFEKL by endogenous processing is prohibited. In order to fulfill this condition, we constructed the corresponding viruses mCMV-SIINFEKA and mCMV-Δ*m06m152*-SIINFEKA, in which the SIINFEKL epitope is selectively deleted by the point mutation L174A at the C-terminal K^b anchor position of the antigenic peptide. Thus, these "epitopeless" control viruses can be used to provide all influences of infection except endogenous delivery of the peptide under study.

With this specifically devised approach, we have learned that after endogenous antigen processing in the absence of immunoevasins, as many as 10% of all cell surface K^b molecules can present a single antigenic peptide encoded by a complex virus such as mCMV, with a coding capacity of ~170 open reading frames (69, 83). This is an enormous proportion if we consider the likely competition among a multitude of "self" peptides and viral peptides for the same presenting MHC-I molecule (17). It is important that the high K^b occupancy level by SIINFEKL is not overestimated by potential cross-recognition of other viral or cellular K^b- or D^b-peptide complexes, so-called mimotopes (11, 81), since MAb T-AG 25-D1-16 did not detect any noncognate pMHC complexes at the surfaces of uninfected cells or cells infected with the specificity control viruses mCMV-SIINFEKA and mCMV-Δ*m06m152*-SIINFEKA, which encode all viral epitopes with the exception of the reporter peptide SIINFEKL (Fig. 6B and 7B). Notably, with a K^b occupancy of only 1%, exogenous loading after infection with mCMV-Δ*m06m152*-SIINFEKA proved to be 10-fold less efficient than endogenous loading by infection with mCMV-Δ*m06m152*-SIINFEKL, even if an unphysiologically high dose of SIINFEKL peptide (10^{-4} M) was used for exogenous loading.

The superiority of endogenous loading may be explained by a high efficiency of chaperone-assisted peptide loading onto nascent MHC-I molecules in a specific loading complex in the ER (reviewed in reference 13), whereas exogenous loading requires replacement of already bound "self" or viral peptides by affinity-dependent peptide competition (59). Although SIINFEKL was found to bind with high affinity to K^b, resulting in very stable K^b-SIINFEKL complexes (8, 30), its dissociation constant may nevertheless be too high to replace viral peptides of even higher affinity (44). Interestingly, for uninfected cells in which MHC-I molecules present only "self" peptides, exogenous loading reached a K^b occupancy close to the values reached by endogenous loading after infection in the absence of immunoevasins. It should be noted, however, that K^b occupancy by the ligand SIINFEKL also correlated with the cell surface expression density of its receptor K^b (Fig. 7). Regardless of which of the two explanations applies, endogenous loading is highly efficient.

It is worthwhile to compare here the observed MHC-I occupancy with the experience seen in other systems (for a list, see reference 82). The numbers of pMHC complexes displayed at the cell surface were found to differ largely, with the highest number being ~10^4 complexes, corresponding to an MHC-I occupancy of 10%, reported for the K^d-restricted peptide SYFPEITHI, derived from the JAK-1 tyrosine kinase of P815 mastocytoma cells (16, 68). Thus, the K^b occupancy of 10% by SIINFEKL observed here in the absence of immunoevasins belongs to the top flight in the ranking. SIINFEKL, however, is also a splendid example for highlighting the importance of the expression and detection systems. Specifically, Rötzschke et al. (78) reported a total number of only ~100 K^b-SIINFEKL complexes in lysates of Ova-transfected cells, which predicts an even smaller number at the cell surface. Using MAb T-AG

25-D1-16 for the detection of cell surface K^b-SIINFEKL complexes, Porgador et al. (65) found an occupancy of ~9% after infection of L-K^b cells with the recombinant vaccinia virus VV-Ova, expressing full-length Ova, whereas occupancies of up to 86% were reached after infection with recombinant vaccinia viruses carrying different constructs of SIINFEKL minigenes.

Our studies were not aimed at developing an optimal vector for expressing SIINFEKL but at studying the role of mCMV immunoevasins in epitope presentation during a largely untouched viral replication cycle. This was the rationale for inserting just the SIINFEKL sequence in place of an intrinsic antigenic peptide of a viral carrier protein. The observed K^b occupancy of 10% by SIINFEKL after endogenous loading in the absence of immunoevasins is particularly impressive in view of the long list of K^b-restricted mCMV intrinsic epitopes identified by Munks and colleagues (55), which includes some of the most immunodominant antigenic peptides of the acute immune response to mCMV in the H-2^b haplotype, such as the m139, M57, m141, M38, and M78 epitopes (54). As shown in Fig. 4A, SIINFEKL expressed in the gp36.5/m164 carrier protein takes an only intermediate position in the immunodominance hierarchy of H-2^b-restricted mCMV peptides. However, this does not necessarily imply an even higher MHC-I occupancy by the higher-ranking peptides, since recent studies have indicated that the magnitude of the primary immune response to particular epitopes, which defines epitope immunodominance, is primarily determined by the TCR specificity repertoire of the naïve precursor cell pool (23, 57, 86).

In the presence of immunoevasins after infection with mCMV-SIINFEKL, in addition to an absolute reduction in the number of K^b molecules as well as K^b-SIINFEKL complexes, the K^b occupancy by SIINFEKL declined to <1% in relative terms (Fig. 6B). Interestingly, the efficiency of cognate CD8 T-cell priming (Fig. 4B) did not at all positively correlate with K^b occupancy by SIINFEKL in infected cells; rather, priming with mCMV-SIINFEKL was somewhat more efficient than priming with mCMV-Δ*m06m152*-SIINFEKL, despite the much lower K^b occupancy. This finding is in accordance with the previous notion that viral immunoevasins expressed in infected cells do not influence epitope immunodominance hierarchies (21, 36, 56, 71), most probably because priming is mediated through epitope cross-presentation by uninfected dendritic cells rather than through direct presentation by infected cells (7, 25, 26, 88, 94). The paradox of improved priming in the presence of immunoevasins was explained recently by the "negative feedback model" of CD8 T-cell priming. According to this model, inhibition of epitope presentation by immunoevasins protects infected cells in the lymph node cortex against attack by recently primed effector CD8 T cells, with the consequence of enhanced virus replication associated with enhanced delivery of viral antigenic proteins for sustained cross-priming (5).

Importantly, immunoevasins were found to affect total cell surface K^b and endogenously generated K^b-SIINFEKL complexes differentially. Specifically, 16 h after infection, cells infected with mCMV-Δ*m06m152*-SIINFEKL displayed 1×10^5 K^b molecules at the cell surface, a number which was reduced by a factor of ~3, namely, to 3×10^4 K^b molecules, in the presence of immunoevasins after infection with mCMV-SIINFEKL. In contrast, the reduction was 50-fold for K^b-SIINFEKL complexes, namely, from 1×10^4 complexes in the absence of immunoevasins to 200 (with all numbers representing median values) in their presence. Since all MHC-I molecules trafficking to the cell surface are thought to actually be loaded with a peptide (2), and since immunoevasins should target all K^b-peptide complexes with similar affinities, and not preferentially the K^b-SIINFEKL complexes, one rather might have expected a comparable effect of immunoevasins on all K^b molecules and K^b-SIINFEKL complexes. It was reasonable, therefore, to hypothesize that immunoevasins affect exclusively, or at least primarily, the transport of recently loaded pMHC complexes to the cell surface and that pMHC complexes already present at the cell surface are not directly affected. The undisputed decline in steady-state levels of cell surface MHC-I over time (89) could possibly be explained by an indirect effect of immunoevasins, namely, by blocking the resupply of new pMHC complexes after constitutive MHC-I endocytosis.

To test this hypothesis, we compared the fate of preexisting cell surface K^b molecules, whose intrinsically presented antigenic peptides were replaced with SIINFEKL by exogenous peptide loading, with the fate of endogenously generated K^b-SIINFEKL complexes. An advantage of this approach is that recently loaded and preexisting pMHC complexes under investigation are molecularly identical, so the affinity of interaction between immunoevasins and the pMHC complexes is no longer a variable in the comparison. The results were pretty clear in demonstrating a preferential effect of immunoevasins on newly generated K^b-SIINFEKL complexes.

Previous work by Wagner and colleagues (89), using simian virus 40 (SV40)-transformed H-2^b and H-2^d MEF cell lines for infection, has shown that cell surface expression of K^b is least affected by mCMV immunoevasins, with an allele ranking in cell surface downmodulation of $K^d \sim D^d \sim D^b > L^d \gg K^b$. At the time of that work, it was absolutely logical to propose MHC allele-specific differences in the efficacy of immunoevasins, and biochemical data supported this view by showing less efficient ER retention of newly synthesized K^b molecules than D^b molecules (42). Thus, viewed critically, one might argue that having here selected a K^b-presented peptide, such as SIINFEKL, for studying mCMV immunoevasin function was the worst possible choice. On the other hand, however, using the same set of immune evasion gene deletion mutants used already by Wagner and colleagues, immunoevasins were found to almost completely inhibit K^b-peptide presentation to cognate CD8 T cells after endogenous loading in infected cells (34, 62). This accordant finding from two independent groups was difficult to explain in view of the biochemical data indicating escape of K^b molecules from ER retention, since only a few pMHC complexes must reach the cell surface for sensitization of CD8 T cells. The evidence for K^b molecules passing the Golgi apparatus in the presence of immunoevasins did not formally exclude the possibility that peptide presentation at the cell surface is inhibited by gp48/m06-mediated lysosomal degradation or by complex formation with gp34/m04. This explanation, however, does not apply either, since solitary expression of gp40/m152 in the mutant virus mCMV-Δ*m04m06* was found to strongly inhibit the presentation of K^b-presented peptides (34).

Our data now offer a new interpretation to resolve this

alleged conflict in the literature. While endogenous presentation of K^b-SIINFEKL was found in this study to already be inhibited strongly by immunoevasins at 8 h postinfection, preexisting cell surface-resident K^b molecules as well as exogenously loaded K^b-SIINFEKL complexes were barely affected at that time point, and this might have also been the case in the study by Wagner and colleagues, in which cytofluorometric detection of cell surface K^b was performed at 12 h postinfection (89). Our finding that cell surface K^b is significantly downmodulated at 16 h postinfection but not yet at 8 h postinfection is in reasonable accordance with the cell surface half-life of ~9 h determined for K^b-SIINFEKL complexes in the work by Chefalo and Harding (8). Thus, MHC allele-specific differences in steady-state cell surface expression in the presence of immunoevasins, which interrupt trafficking of new MHC-I molecules to the cell surface, might reflect differences in the constitutive turnover rates of different class I allomorphs rather than a differential molecular susceptibility to mCMV immunoevasins. Accordingly, under the influence of immunoevasins, MHC-I allomorphs with high and low turnover rates are predicted to be downmodulated faster and slower, respectively. Clearly, such a mechanism can explain why the impact of immunoevasins on cell surface class I expression does not correlate directly with their impact on T-cell recognition.

It has been concluded from previous work that m06 and m152 cooperate in preventing MHC-I transport to the cell surface, although the data indicated differential effects after their solitary expression in that m06 proved to be somewhat more efficient in the downmodulation of cell surface MHC-I, while m152 was more efficient in inhibiting peptide presentation. This was revealed by comparing infections with viruses mCMV-Δ*m04m152* and mCMV-Δ*m04m06*, which express m06 and m152, respectively. As an additional layer of complication, gp34/m04 plays a still enigmatic role in these processes, even though its solitary expression in mCMV-Δ*m06m152* does not downmodulate cell surface MHC-I or inhibit peptide presentation (34, 62, 89). We first focused here on describing the concerted impact of the verified immunoevasins m06 and m152 in the presence of m04, but we prudently cloned m164-SIINFEKL into a shuttle vector, so the reporter peptide can easily be expressed in other BAC-cloned mutants to study, for instance, the differential effects of m06 and m152 on K^b and K^b-SIINFEKL cell surface expression as well as their proposed interplay with m04. It is apparent, however, that this approach should ideally be complemented with functional studies and has the limitation that it cannot address differences imposed by MHC polymorphism and epitope variety. On the other hand, it is open for wider application with any BAC-cloned mCMV mutant of interest.

In conclusion, these data have shown that mCMV immunoevasins operate primarily by inhibiting the cell surface transport of recently generated pMHC complexes and thus only indirectly downmodulate MHC-I cell surface expression by interfering with MHC-I turnover at the stage of resupply.

ACKNOWLEDGMENTS

This research was conducted by Niels A. W. Lemmermann in partial fulfillment of the requirements for a doctoral degree from Philipps University, Marburg, Germany.

We thank the Confocal Laser Scanning Microscopy Core Facility of the Forschungszentrum Immunologie (FZI) of the Johannes Gutenberg University for assistance with image collection and the Central Laboratory Animal Facility (CLAF) team for animal care.

Extramural support was provided by the Deutsche Forschungsgemeinschaft, Clinical Research Group KFO 183, for individual project TP8 ("Establishment of a Challenge Model for Optimizing the Immunotherapy of Cytomegalovirus Disease") (N.A.W.L., K.G., P.D., and M.J.R.), and Collaborative Research Center SFB 490, for individual project E4 ("Antigen Presentation under the Influence of Murine Cytomegalovirus Immunoevasins") (V.B., T.D., and M.J.R.). Intramural support was provided to N.A.W.L. by the MAIFOR Young Investigators Program (2007; project no. 10) of the University Medical Center of the Johannes Gutenberg University Mainz.

REFERENCES

1. **Alcami, A., and U. H. Koszinowski.** 2000. Viral mechanisms of immune evasion. Immunol. Today **9:**447–455.
2. **Attaya, M., S. Jameson, C. K. Martinez, E. Hermel, C. Aldrich, J. Forman, K. F. Lindahl, M. J. Bevan, and J. J. Monaco.** 1992. Ham-2 corrects the class I antigen-processing defect in RMA-S cells. Nature **355:**647–649.
3. **Böhm, V., J. Podlech, D. Thomas, P. Deegen, M. F. Pahl-Seibert, N. A. Lemmermann, N. K. Grzimek, S. A. Oehrlein-Karpi, M. J. Reddehase, and R. Holtappels.** 2008. Epitope-specific in vivo protection against cytomegalovirus disease by CD8 T cells in the murine model of preemptive immunotherapy. Med. Microbiol. Immunol. **197:**135–144.
4. **Böhm, V., C. K. Seckert, C. O. Simon, D. Thomas, A. Renzaho, D. Gendig, R. Holtappels, and M. J. Reddehase.** 2009. Immune evasion proteins enhance cytomegalovirus latency in the lungs. J. Virol. **83:**10293–10298.
5. **Böhm, V., C. O. Simon, J. Podlech, C. K. Seckert, D. Gendig, P. Deegen, D. Gillert-Marien, N. A. Lemmermann, R. Holtappels, and M. J. Reddehase.** 2008. The immune evasion paradox: immunoevasins of murine cytomegalovirus enhance priming of CD8 T cells by preventing negative feedback regulation. J. Virol. **82:**11637–11650.
6. **Borst, E. M., G. Posfai, F. Pogoda, and M. Messerle.** 2004. Mutagenesis of herpesvirus BACs by allele replacement. Methods Mol. Biol. **256:**269–279.
7. **Carbone, F. R., and M. J. Bevan.** 1990. Class I-restricted processing and presentation of exogenous cell-associated antigen in vivo. J. Exp. Med. **171:**377–387.
8. **Chefalo, P. J., and C. V. Harding.** 2001. Processing of exogenous antigens for presentation by class I MHC molecules involves post-Golgi peptide exchange influenced by peptide-MHC complex stability and acidic pH. J. Immunol. **167:**1274–1282. (Erratum, **170:**643, 2003.)
9. **Cobbold, M., N. Khan, B. Pourgheysari, S. Tauro, D. McDonald, H. Osman, M. Assenmacher, I. Billingham, C. Steward, C. Crawley, E. Olavarria, J. Goldman, R. Chakraverty, P. Mahendra, C. Craddock, and P. A. Moss.** 2005. Adoptive transfer of cytomegalovirus-specific CTL to stem cell transplant patients after selection by HLA-peptide tetramers. J. Exp. Med. **202:**379–386.
10. **Cohen, C. J., G. Denkberg, A. Lev, M. Epel, and Y. Reiter.** 2003. Recombinant antibodies with MHC-restricted, peptide-specific, T-cell receptor-like specificity: new tools to study antigen presentation and TCR-peptide-MHC interactions. J. Mol. Recognit. **16:**324–332.
11. **Crawford, F., E. Huseby, J. White, P. Marrack, and J. W. Kappler.** 2004. Mimotopes for alloreactive and conventional T cells in a peptide-MHC display library. PLoS Biol. **2:**E90.
12. **Denkberg, G., and Y. Reiter.** 2006. Recombinant antibodies with T-cell receptor-like specificity: novel tools to study MHC class I presentation. Autoimmun. Rev. **5:**252–257.
13. **Donaldson, J. G., and D. B. Williams.** 2009. Intracellular assembly and trafficking of MHC class I molecules. Traffic **10:**1745–1752.
14. **Doom, C. M., and A. B. Hill.** 2008. MHC class I immune evasion in MCMV infection. Med. Microbiol. Immunol. **197:**191–204.
15. **Eberl, G., C. Widmann, and G. Corradin.** 1996. The functional half-life of H-2Kd-restricted T cell epitopes on living cells. Eur. J. Immunol. **26:**1993–1999.
16. **Falk, K., O. Rötzschke, S. Stevanović, G. Jung, and H. G. Rammensee.** 1991. Allele-specific motifs revealed by sequencing of self-peptides eluted from MHC molecules. Nature **351:**290–296.
17. **Fortier, M. H., E. Caron, M. P. Hardy, G. Voisin, S. Lemieux, C. Perreault, and P. Thibault.** 2008. The MHC class I peptide repertoire is molded by the transcriptome. J. Exp. Med. **205:**595–610.
18. **Geginat, G., T. Ruppert, H. Hengel, R. Holtappels, and U. H. Koszinowski.** 1997. IFN-gamma is a prerequisite for optimal antigen processing of viral peptides in vivo. J. Immunol. **158:**3303–3310.
19. **Ghazal, P., M. Messerle, K. Osborn, and A. Angulo.** 2003. An essential role of the enhancer for murine cytomegalovirus in vivo growth and pathogenesis. J. Virol. **77:**3217–3228.
20. **Ghazal, P., A. E. Visser, M. Gustems, R. García, E. M. Borst, K. Sullivan, M. Messerle, and A. Angulo.** 2005. Elimination of IE1 significantly attenuates

murine cytomegalovirus virulence but does not alter replicative capacity in cell culture. J. Virol. **79:**7182–7194.
21. **Gold, M. C., M. W. Munks, M. Wagner, U. H. Koszinowski, A. B. Hill, and S. P. Fling.** 2002. The murine cytomegalovirus immunomodulatory gene *m152* prevents recognition of infected cells by M45-specific CTL but does not alter the immunodominance of the M45-specific CD8 T cell response in vivo. J. Immunol. **169:**359–365.
22. **Gold, M. C., M. W. Munks, M. Wagner, C. W. McMahon, A. Kelly, D. G. Kavanagh, M. K. Slifka, U. H. Koszinowski, D. H. Raulet, and A. B. Hill.** 2004. Murine cytomegalovirus interference with antigen presentation has little effect on the size or the effector memory phenotype of the CD8 T cell response. J. Immunol. **172:**6944–6953.
23. **Haluszczak, C., A. D. Akue, S. E. Hamilton, L. D. Johnson, L. Pujanauski, L. Teodorovic, S. C. Jameson, and R. M. Kedl.** 2009. The antigen-specific CD8+ T cell repertoire in unimmunized mice includes memory phenotype cells bearing markers of homeostatic expansion. J. Exp. Med. **206:**435–448.
24. **Hansen, T. H., and M. Bouvier.** 2009. MHC class I antigen presentation: learning from viral evasion strategies. Nat. Rev. Immunol. **9:**503–513.
25. **Heath, W. R., and F. R. Carbone.** 2001. Cross-presentation in viral immunity and self-tolerance. Nat. Rev. Immunol. **1:**126–134.
26. **Heath, W. R., and F. R. Carbone.** 2001. Cross-presentation, dendritic cells, tolerance and immunity. Annu. Rev. Immunol. **19:**47–64.
27. **Hengel, H., W. Brune, and U. H. Koszinowski.** 1998. Immune evasion by cytomegalovirus—survival strategies of a highly adapted opportunist. Trends Microbiol. **6:**190–197.
28. **Hengel, H., P. Lucin, S. Jonjić, T. Ruppert, and U. H. Koszinowski.** 1994. Restoration of cytomegalovirus antigen presentation by gamma interferon combats viral escape. J. Virol. **68:**289–297.
29. **Hengel, H., U. Reusch, A. Gutermann, H. Ziegler, S. Jonjic, P. Lucin, and U. H. Koszinowski.** 1999. Cytomegaloviral control of MHC class I function in the mouse. Immunol. Rev. **168:**167–176.
30. **Hilton, C. J., A. M. Dahl, and K. L. Rock.** 2001. Anti-peptide antibody blocks peptide binding to MHC class I molecules in the endoplasmic reticulum. J. Immunol. **166:**3952–3956.
31. **Ho, S. N., H. D. Hunt, R. M. Horton, J. K. Pullen, and L. R. Pease.** 1989. Site-directed mutagenesis by overlap extension using the polymerase chain reaction. Gene **77:**51–59.
32. **Hogquist, K. A., M. A. Gavin, and M. J. Bevan.** 1993. Positive selection of CD8+ T cells induced by major histocompatibility complex binding peptides in fetal thymic organ culture. J. Exp. Med. **177:**1469–1473.
33. **Holtappels, R., V. Böhm, J. Podlech, and M. J. Reddehase.** 2008. CD8 T-cell-based immunotherapy of cytomegalovirus infection: "proof of concept" provided by the murine model. Med. Microbiol. Immunol. **197:**125–134.
34. **Holtappels, R., D. Gillert-Marien, D. Thomas, J. Podlech, P. Deegen, S. Herter, S. A. Oehrlein-Karpi, D. Strand, M. Wagner, and M. J. Reddehase.** 2006. Cytomegalovirus encodes a positive regulator of antigen presentation. J. Virol. **80:**7613–7624.
35. **Holtappels, R., N. K. Grzimek, C. O. Simon, D. Thomas, D. Dreis, and M. J. Reddehase.** 2002. Processing and presentation of murine cytomegalovirus pORFm164-derived peptide in fibroblasts in the face of all viral immunosubversive early gene functions. J. Virol. **76:**6044–6053.
36. **Holtappels, R., M. W. Munks, J. Podlech, and M. J. Reddehase.** 2006. CD8 T-cell-based immunotherapy of cytomegalovirus disease in the mouse model of the immunocompromised bone marrow transplantation recipient, p. 383–418. *In* M. J. Reddehase (ed.), Cytomegaloviruses: molecular biology and immunology. Caister Academic Press, Wymondham, Norfolk, United Kingdom.
37. **Holtappels, R., J. Podlech, M. F. Pahl-Seibert, M. Jülch, D. Thomas, C. O. Simon, M. Wagner, and M. J. Reddehase.** 2004. Cytomegalovirus misleads its host by priming of CD8 T cells specific for an epitope not presented in infected tissues. J. Exp. Med. **199:**131–136.
38. **Holtappels, R., C. O. Simon, M. W. Munks, D. Thomas, P. Deegen, B. Kühnapfel, T. Däubner, S. F. Emde, J. Podlech, N. K. Grzimek, S. A. Oehrlein-Karpi, A. B. Hill, and M. J. Reddehase.** 2008. Subdominant CD8 T-cell epitopes account for protection against cytomegalovirus independent of immunodomination. J. Virol. **82:**5781–5796.
39. **Holtappels, R., D. Thomas, J. Podlech, and M. J. Reddehase.** 2002. Two antigenic peptides from genes *m123* and *m164* of murine cytomegalovirus quantitatively dominate CD8 T-cell memory in the H-2^d haplotype. J. Virol. **76:**151–164.
40. **Holtappels, R., D. Thomas, and M. J. Reddehase.** 2009. The efficacy of antigen processing is critical for protection against cytomegalovirus disease in the presence of viral immune evasion proteins. J. Virol. **83:**9611–9615.
41. **Hudson, J. B., V. Misra, and T. R. Mosmann.** 1976. Cytomegalovirus infectivity: analysis of the phenomenon of centrifugal enhancement of infectivity. Virology **72:**235–243.
42. **Kavanagh, D. G., M. C. Gold, M. Wagner, U. H. Koszinowski, and A. B. Hill.** 2001. The multiple immune-evasion genes of murine cytomegalovirus are not redundant: m4 and m152 inhibit antigen presentation in a complementary and cooperative fashion. J. Exp. Med. **194:**967–977.
43. **Kern, M., A. Popov, K. Scholz, B. Schumak, D. Djandji, A. Limmer, D. Eggle, T. Sacher, R. Zawatzky, R. Holtappels, M. J. Reddehase, G. Hartmann, S. Debey-Pascher, L. Diehl, U. Kalinke, U. Koszinowski, J. Schultze, and P. Knolle.** 2009. Virally infected mouse liver endothelial cells trigger CD8+ T-cell immunity. Gastroenterology doi:10.1053/j.gastro.2009.08.057.
44. **Khilko, S. N., M. T. Jelonek, M. Corr, L. F. Boyd, A. L. Bothwell, and D. H. Margulies.** 1995. Measuring interactions of MHC class I molecules using surface plasmon resonance. J. Immunol. Methods **183:**77–94.
45. **Kielczewska, A., M. Pyzik, T. Sun, A. Krmpotic, M. B. Lodoen, M. W. Munks, M. Babic, A. B. Hill, U. H. Koszinowski, S. Jonjic, L. L. Lanier, and S. M. Vidal.** 2009. Ly49P recognition of cytomegalovirus-infected cells expressing H2-D^k and CMV-encoded m04 correlates with the NK cell antiviral response. J. Exp. Med. **206:**515–523.
46. **Kleijnen, M. F., J. B. Huppa, P. Lucin, S. Mukherjee, H. Farrell, A. E. Campbell, U. H. Koszinowski, A. B. Hill, and H. Ploegh.** 1997. A mouse cytomegalovirus glycoprotein, gp34, forms a complex with folded class I MHC molecules in the ER which is not retained but is transported to the cell surface. EMBO J. **16:**685–694.
47. **Krmpotic, A., D. H. Busch, I. Bubic, F. Gebhardt, H. Hengel, M. Hasan, A. A. Scalzo, U. H. Koszinowski, and S. Jonjic.** 2002. MCMV glycoprotein gp40 confers virus resistance to CD8$^+$ T lymphocytes and NK cells in vivo. Nat. Immunol. **3:**529–535.
48. **Krmpotic, A., M. Messerle, I. Crnkovic-Mertens, B. Polic, S. Jonjic, and U. H. Koszinowski.** 1999. The immunoevasive function encoded by the mouse cytomegalovirus gene *m152* protects the virus against T cell control in vivo. J. Exp. Med. **190:**1285–1295.
49. **Kurz, S. K., H.-P. Steffens, A. Mayer, J. R. Harris, and M. J. Reddehase.** 1997. Latency versus persistence or intermittent recurrences: evidence for a latent state of murine cytomegalovirus in the lungs. J. Virol. **71:**2980–2987.
50. **Lilley, B. N., and H. L. Ploegh.** 2005. Viral modulation of antigen presentation: manipulation of cellular targets in the ER and beyond. Immunol. Rev. **207:**126–144.
51. **Lu, X., A. K. Pinto, A. M. Kelly, K. S. Cho, and A. B. Hill.** 2006. Murine cytomegalovirus interference with antigen presentation contributes to the inability of CD8 T cells to control virus in the salivary gland. J. Virol. **80:**4200–4202.
52. **Mahmutefendić, H., G. Blagojević, N. Kucić, and P. Lucin.** 2007. Constitutive internalization of murine MHC class I molecules. J. Cell. Physiol. **210:**445–455.
53. **Messerle, M., I. Crnkovic, W. Hammerschmidt, H. Ziegler, and U. H. Koszinowski.** 1997. Cloning and mutagenesis of a herpesvirus genome as an infectious bacterial artificial chromosome. Proc. Natl. Acad. Sci. USA **94:**14759–14763.
54. **Munks, M. W., K. S. Cho, A. K. Pinto, S. Sierro, P. Klenerman, and A. B. Hill.** 2006. Four distinct patterns of memory CD8 T cell responses to chronic murine cytomegalovirus infection. J. Immunol. **177:**450–458.
55. **Munks, M. W., M. C. Gold, A. L. Zajac, C. M. Doom, C. S. Morello, D. H. Spector, and A. B. Hill.** 2006. Genome-wide analysis reveals a highly diverse CD8 T cell response to murine cytomegalovirus. J. Immunol. **176:**3760–3766.
56. **Munks, M. W., A. K. Pinto, C. M. Doom, and A. B. Hill.** 2007. Viral interference with antigen presentation does not alter acute or chronic CD8 T cell immunodominance in murine cytomegalovirus infection. J. Immunol. **178:**7235–7241.
57. **Obar, J. J., K. M. Khanna, and L. Lefrançois.** 2008. Endogenous naive CD8+ T cell precursor frequency regulates primary and memory responses to infection. Immunity **28:**859–869.
58. **O'Connor, M., M. Peifer, and W. Bender.** 1989. Construction of large DNA segments in *Escherichia coli*. Science **244:**1307–1312.
59. **Ojcius, D. M., J. P. Abastado, A. Casrouge, E. Mottez, L. Cabanie, and P. Kourilsky.** 1993. Dissociation of the peptide-MHC class I complex limits the binding rate of exogenous peptide. J. Immunol. **151:**6020–6026.
60. **Pahl-Seibert, M.-F., M. Juelch, J. Podlech, D. Thomas, P. Deegen, M. J. Reddehase, and R. Holtappels.** 2005. Highly protective in vivo function of cytomegalovirus IE1 epitope-specific memory CD8 T cells purified by T-cell receptor-based cell sorting. J. Virol. **79:**5400–5413.
61. **Peggs, K. S., S. Verfuerth, A. Pizzey, N. Khan, M. Gulver, P. A. Moss, and S. Mackinnon.** 2003. Adoptive cellular therapy for early cytomegalovirus infection after allogeneic stem-cell transplantation with virus-specific T-cell lines. Lancet **362:**1375–1377.
62. **Pinto, A. K., M. W. Munks, U. H. Koszinowski, and A. B. Hill.** 2006. Coordinated function of murine cytomegalovirus genes completely inhibits CTL lysis. J. Immunol. **177:**3225–3234.
63. **Ploegh, H.** 1998. Viral strategies of immune evasion. Science **280:**248–253.
64. **Podlech, J., R. Holtappels, N. K. A. Grzimek, and M. J. Reddehase.** 2002. Animal models: murine cytomegalovirus, p. 493–525. *In* S. H. E. Kaufmann and D. Kabelitz (ed.), Methods in microbiology: immunology of infection, 2nd ed., vol. 32. Academic Press, London, United Kingdom.
65. **Porgador, A., J. W. Yewdell, Y. Deng, J. R. Bennink, and R. N. Germain.** 1997. Localization, quantitation, and in situ detection of specific peptide-MHC class I complexes using a monoclonal antibody. Immunity **6:**715–726.
66. **Posfai, G., M. D. Koob, H. A. Kirkpatrick, and F. R. Blattner.** 1997. Versatile insertion plasmids for targeted genome manipulations in bacteria: isolation,

deletion, and rescue of the pathogenicity island LEE of the *Escherichia coli* O157:H7 genome. J. Bacteriol. **179:**4426–4428.
67. **Quinnan, G. V., Jr., W. H. Burns, N. Kirmani, A. H. Rook, J. Manischewitz, L. Jackson, G. W. Santos, and R. Sarai.** 1984. HLA-restricted cytotoxic T lymphocytes are an early immune response and important defense mechanism in cytomegalovirus infections. Rev. Infect. Dis. **6:**156–163.
68. **Rammensee, H. G., K. Falk, and O. Rötzschke.** 1993. MHC molecules as peptide receptors. Curr. Opin. Immunol. **5:**35–44.
69. **Rawlinson, W. D., H. E. Farrell, and B. G. Barrell.** 1996. Analysis of the complete DNA sequence of murine cytomegalovirus. J. Virol. **70:**8833–8849.
70. **Reddehase, M. J.** 2002. Antigens and immunoevasins: opponents in cytomegalovirus immune surveillance. Nat. Rev. Immunol. **2:**831–844.
71. **Reddehase, M. J., C. O. Simon, J. Podlech, and R. Holtappels.** 2004. Stalemating a clever opportunist: lessons from murine cytomegalovirus. Hum. Immunol. **65:**446–455.
72. **Reddehase, M. J., F. Weiland, K. Münch, S. Jonjic, A. Lüske, and U. H. Koszinowski.** 1985. Interstitial murine cytomegalovirus pneumonia after irradiation: characterization of cells that limit viral replication during established infection of the lungs. J. Virol. **55:**264–273.
73. **Reusch, U., O. Bernhard, U. Koszinowski, and P. Schu.** 2002. AP-1A and AP-3A lysosomal sorting functions. Traffic **3:**752–761.
74. **Reusch, U., W. Muranyi, P. Lucin, H. G. Burgert, H. Hengel, and U. H. Koszinowski.** 1999. A cytomegalovirus glycoprotein re-routes MHC class I complexes to lysosomes for degradation. EMBO J. **18:**1081–1091.
75. **Reusser, P., S. R. Riddell, J. D. Meyers, and P. D. Greenberg.** 1991. Cytotoxic T-lymphocyte response to cytomegalovirus after human allogeneic bone marrow transplantation: pattern of recovery and correlation with cytomegalovirus infection and disease. Blood **78:**1373–1380.
76. **Riddell, S. R., K. S. Watanabe, J. M. Goodrich, C. R. Li, M. E. Agha, and P. D. Greenberg.** 1992. Restoration of viral immunity in immunodeficient humans by the adoptive transfer of T cell clones. Science **257:**238–241.
77. **Rock, K. L., and A. L. Goldberg.** 1999. Degradation of cell proteins and the generation of MHC class I-presented peptides. Annu. Rev. Immunol. **17:**739–779.
78. **Rötzschke, O., K. Falk, S. Stevanović, G. Jung, P. Walden, and H. G. Rammensee.** 1991. Exact prediction of a natural T cell epitope. Eur. J. Immunol. **21:**2891–2894.
79. **Simon, C. O., R. Holtappels, H.-M. Tervo, V. Böhm, T. Däubner, S. A. Oehrlein-Karpi, B. Kühnapfel, A. Renzaho, D. Strand, J. Podlech, M. J. Reddehase, and N. K. A. Grzimek.** 2006. CD8 T cells control cytomegalovirus latency by epitope-specific sensing of transcriptional reactivation. J. Virol. **80:**10436–10456.
80. **Snyder, C. M., K. S. Cho, E. L. Bonnett, S. van Dommelen, G. R. Shellam, and A. B. Hill.** 2009. Memory inflation during chronic viral infection is maintained by continuous production of short-lived, functional T cells. Immunity **29:**65065–65069.
81. **Sparbier, K., and P. Walden.** 1999. T cell receptor specificity and mimotopes. Curr. Opin. Immunol. **11:**214–218.
82. **Stevanović, S., and H. Schild.** 1999. Quantitative aspects of T cell activation-peptide generation and editing by MHC class I molecules. Semin. Immunol. **11:**375–384.
83. **Tang, Q., E. A. Murphy, and G. G. Maul.** 2006. Experimental confirmation of global murine cytomegalovirus open reading frames by transcriptional detection and partial characterization of newly described gene products. J. Virol. **80:**6873–6882.
84. **Tortorella, D., B. E. Gewurz, M. H. Furman, D. J. Schust, and H. L. Ploegh.** 2000. Viral subversion of the immune system. Annu. Rev. Immunol. **18:**861–926.
85. **Townsend, A. R., J. Rothbard, F. M. Gotch, G. Bahadur, D. Wraith, and A. J. McMichael.** 1986. The epitopes of influenza nucleoprotein recognized by cytotoxic T lymphocytes can be defined with short synthetic peptides. Cell **44:**959–968.
86. **van Heijst, J. W., C. Gerlach, E. Swart, D. Sie, C. Nunes-Alves, R. M. Kerkhoven, R. Arens, M. Correia-Neves, K. Schepers, and T. N. Schumacher.** 2009. Recruitment of antigen-specific CD8+ T cells in response to infection is markedly efficient. Science **325:**1265–1269.
87. **van Kaer, L.** 2002. Major histocompatibility complex class I-restricted antigen processing and presentation. Tissue Antigens **60:**1–9.
88. **Villadangos, J. A., W. R. Heath, and F. R. Carbone.** 2007. Outside looking in: the inner workings of the cross-presentation pathways within dendritic cells. Trends Immunol. **28:**45–47.
89. **Wagner, M., A. Gutermann, J. Podlech, M. J. Reddehase, and U. H. Koszinowski.** 2002. MHC class I allele-specific cooperative and competitive interactions between immune evasion proteins of cytomegalovirus. J. Exp. Med. **196:**805–816.
90. **Wagner, M., S. Jonjic, U. H. Koszinowski, and M. Messerle.** 1999. Systematic excision of vector sequences from the BAC-cloned herpesvirus genome during virus reconstitution. J. Virol. **73:**7056–7060.
91. **Wilhelmi, V., C. O. Simon, J. Podlech, V. Böhm, T. Däubner, S. Emde, D. Strand, A. Renzaho, N. A. W. Lemmermann, C. K. Seckert, M. J. Reddehase, and N. K. A. Grzimek.** 2008. Transactivation of cellular genes involved in nucleotide metabolism by the regulatory IE1 protein of murine cytomegalovirus is not critical for viral replicative fitness in quiescent cells and host tissues. J. Virol. **82:**9900–9916.
92. **Yewdell, J., L. C. Antón, I. Bacik, U. Schubert, H. L. Snyder, and J. R. Bennink.** 1999. Generating MHC class I ligands from viral gene products. Immunol. Rev. **172:**97–108.
93. **Yewdell, J. W., and J. R. Bennink.** 2001. Cut and trim: generating MHC class I peptide ligands. Curr. Opin. Immunol. **13:**13–18.
94. **Yewdell, J. W., and S. M. Haeryfar.** 2005. Understanding presentation of viral antigens to CD8+ T cells in vivo: the key to rational vaccine design. Annu. Rev. Immunol. **23:**651–682.
95. **Yewdell, J. W., and A. B. Hill.** 2002. Viral interference with antigen presentation. Nat. Immunol. **3:**1019–1025.
96. **Ziegler, H., R. Thale, P. Lucin, W. Muranyi, T. Flohr, H. Hengel, H. Farrell, W. Rawlinson, and U. H. Koszinowski.** 1997. A mouse cytomegalovirus glycoprotein retains MHC class I complexes in the ERGIC/cis-Golgi compartments. Immunity **6:**57–66.
97. **Zinkernagel, R. M., and P. C. Doherty.** 1974. Immunological surveillance against altered self components by sensitised T lymphocytes in lymphocytic choriomeningitis. Nature **251:**547–548.
98. **Zinkernagel, R. M., and P. C. Doherty.** 1974. Restriction of in vitro T cell-mediated cytotoxicity in lymphocytic choriomeningitis within a syngeneic or semiallogeneic system. Nature **248:**701–702.